Laser saturation spectroscopy in the time-delayed mode. Theory of optical free induction decay in coupled Doppler-broadened systems

Martial Ducloy*
Laboratoire de Physique des Lasers, Université Paris-Nord, 93430 Villetaneuse, France

José R. R. Leite† and Michael S. Feld
Department of Physics and Spectroscopy Laboratory, Massachusetts Institute of Technology, Cambridge, Massachusetts 02139
(Received 4 August 1977)

This paper describes a new class of techniques, called time-delayed laser saturation spectroscopy, which combine frequency- and time-domain methods of laser spectroscopy to provide a way of studying a molecular system as it evolves from an initially prepared stationary state to a second, final state. The specific example analyzed here is three-level free induction decay, in which the time-dependent gain of a Doppler-broadened molecular transition is probed after the sudden termination of an intense field resonating with a coupled transition. The theoretical calculation is based on the coupled density-matrix equations of motion in the slowly-varying envelope approximation. The time-delayed line shapes, which may be studied in either transmission or side fluorescence, exhibit linewidth asymmetries, line-shape deformations, Ramsey-type fringes, power broadening and dephasing, and dynamic Stark splittings and oscillatory decays. The technique provides a unique way of distinguishing the influence of Raman-type processes from that of population saturation and a means to separately measure the associated decay rates. The relationship of the present work to other studies is also discussed.

I. INTRODUCTION

Developments over the past decade of powerful techniques in laser spectroscopy for measuring atomic and molecular structure and collisional dynamics in Doppler-broadened gases can be classified in two major categories. On the one hand, steady-state phenomena such as standing-wave saturation[1-3] (Lamb dip) and laser-induced line narrowing[4-6] (three-level) techniques have been used to obtain spectroscopic information in the frequency domain with great precision. On the other hand, coherent transient phenomena such as free-induction decay,[7] optical nutation,[8] and photon echoes[9] have been used in obtaining new information about relaxation processes in the time domain. The main point of this paper is to show that by merging the techniques of these two categories one can combine the advantages of transient and steady-state spectroscopy to extend the range of available information.

To illustrate the new class of techniques, consider a conventional high-resolution spectroscopy experiment in which a tunable monochromatic probe is tuned through a Doppler-broadened transition saturated by an intense monochromatic field to obtain a narrow saturation resonance (Fig. 1). Now suppose that the intense field is suddenly turned off, and the line shape of the narrow resonance is probed a fixed interval of time later. As the time delay is increased the change signal will become smaller, corresponding to the decay of the saturated molecules and their return to equilibrium. Thus, by studying the line shape as a function of delay time a family of curves can be generated. This information can be combined to form a surface in a coordinate system having axes: change-signal intensity (z axis), frequency detuning (x axis), time delay (y axis) (Fig. 2). Sections parallel to the x axis give the change-signal line shape at delayed times. Similarly, sections parallel to the y axis give the free decay of the system at various frequencies. Note that this surface could have equally well been generated from the family of curves obtained from the time decay of the steady-state change signal, holding the probe field fixed at various frequencies.

Studies of this type might well be termed "frequency–time-domain spectroscopy" because both

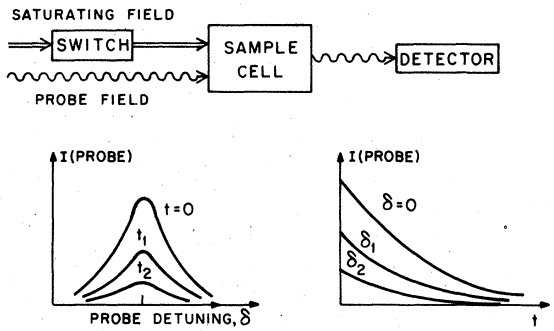

FIG. 1. Simplified setup for time-delayed saturation spectroscopy experiments. The double arrow indicates the saturating field, the wavy arrow the probe field. The saturating field is terminated at time $t = 0$.

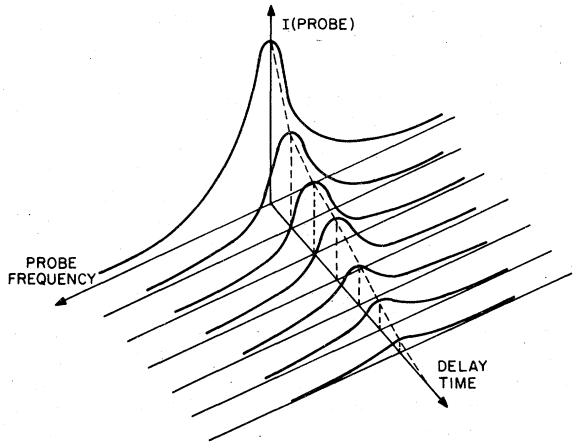

FIG. 2. Three-dimensional representation of the time-delayed change signals.

types of information are obtained simultaneously. As will be seen, such studies extend the possibilities of laser saturation spectroscopy, which only provides information in the frequency domain, as well as those of ordinary coherent transient experiments, which only provide time-domain information.

These time-delayed change signals have some very interesting features. For example, their characteristic decay times may be totally unrelated to the inverse steady-state linewidths. What is more, different portions of the line shape can decay at different rates. Consequently, the *shape* of the narrow resonance can change during the decay process. This behavior occurs because the change signal is composed of contributions arising from different physical processes (population saturation, Raman-type processes, etc.), each of which has a different steady-state linewidth and decays at a different rate. Thus, new physical information not available from the steady-state line shape can be obtained by studying the free decay of the change signal and its line shape as it evolves in time. Other features which can manifest themselves in the time-delayed line shapes include power broadening and dephasing, ac Stark splittings, oscillatory decays, and narrow Ramsey-type resonances.

The time-delayed saturation signals have some features in common with conventional free-induction decay signals observed by means of heterodyne detection using a monochromatic laser field as the local oscillator.[7] In the new technique the probe field acts as a local oscillator to beat with the transient signals induced when the intense field is terminated. However, in this case the probe field also *resonantly interacts* with the saturated molecules, which is not the case in the heterodyne detection of ordinary free-induction decay. It is this interaction which gives rise to the observation of narrow spectral line shapes. In contrast, the ordinary free-induction decay signal is the same, independent of the tuning of the heterodyne laser. This distinction will be made more explicit in what follows.

As is evident from the above discussion, the time decay of the change signal is not simply the Fourier transform of the steady-state line shape. Thus, the present technique is not an analog of Fourier transform spectroscopy,[10] where a computer is used to transform free-induction decay signals and thus obtain a frequency spectrum. One might loosely say that in the new technique the molecules themselves take the transform of the free-decay signals, but it is emphasized that the frequency-domain signals so obtained contain physical information not present in the signals of ordinary free-induction decay. This distinction will be elaborated later on.

The experiment above is one example of a class of time-delayed laser-saturation techniques. Similar behavior will also occur when studying the time-delayed probe line shapes after the intense field is suddenly turned on (analog of optical nutation).[11] The technique is also applicable to studying echoes and other coherent phenomena. Also note that the effects can be studied both in two-level systems and in coupled three-level systems, either by observing the probe transmission or by detecting the side fluorescence from one of the interacting levels. In all cases there are interesting features which depend on whether the probe is co-propagating or counter-propagating with respect to the intense field.

The present paper presents a theoretical analysis of one aspect of this new class of phenomena, three-level free-induction decay, and discusses the new information available, as compared to that obtainable in the usual free-decay and steady-state three-level experiments. In this type of experiment the intense field saturates one transition and the probe field, which may be co- or counter-propagating, acts on a coupled transition (Fig. 3). Both folded [Figs. 3(a) and 3(b)] and cascade [Fig. 3(c)] systems may be studied. This technique pro-

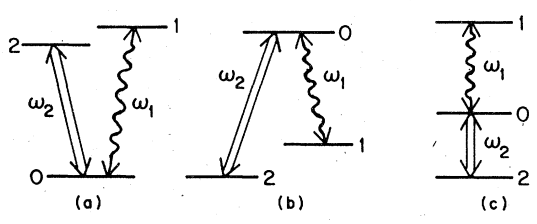

FIG. 3. Energy level diagrams.

vides a novel way of measuring relaxation processes, and a unique means of separating the effects of population saturation from those of Raman-type processes (see below). One application is to describe the transient behavior of optically pumped lasers.

A brief description of the technique and some of the line-shape features of three-level free decay and optical nutation were given in an earlier publication.[12] An experiment which demonstrates the technique in NH_3 will be reported elsewhere.[13]

In this paper, after a discussion of the equations of motion in a three-level system (Sec. II), we calculate the molecular response at the probe frequency for arbitrary intensities of the saturating field (Sec. III) and present a detailed study of the velocity average. The two subsequent sections are devoted to the discussion of the transient response of the probe field in the limits of weak (Sec. IV) and strong (Sec. V) saturating field intensities. Section VI calculates the time evolution of the side fluorescence and compares the results with those obtained for the probe transmission.

Many different symbols will be used throughout this article. To make it easier to read, a glossary of the main symbols is given in Table I.

Before presenting the theoretical analysis, let us mention some relevant previous studies: coherent Raman beats observed in the response of a single electromagnetic (e.m.) field to the sudden Stark splitting of a degenerate transition,[14,15] fluorescence quantum beats induced by pulse excitation,[16] transient two-photon absorption[17,18] and Raman emission,[19] both in the case of a nonresonant intermediate state, and transients in infrared-microwave double resonance.[20] An experiment to study the time-delayed Lamb dip in sodium has also been performed.[21] The connections between some of these works and the present technique will be discussed in the concluding section (Sec. VII).

TABLE I. Glossary of symbols.

	Equation	
$E_1, E_2, \mathcal{E}_1^0, \mathcal{E}_2^0$	(1)	Electromagnetic fields
$g(t), g_0$	(9b), (28a)	Probe gain
$G(v)$	(27)	Velocity distribution
k_1, k_2	(1)	Wave vectors
L_1, L_2, L_{12}	(4)	Resonant frequency denominators
L_B, L_N, L_B^0, L_N^0	(88), (91)	Lorentzian resonance line shapes
$P_1, \mathcal{P}_1$	(8)	Macroscopic polarization
Q	(30)	$\sqrt{1+s}$
s	(19)	Saturation parameter
S	(42b)	High-frequency Stark splitting
u	(27)	Thermal velocity
v_1, v_2, v_{12}^0	(28), (33), (57)	Resonant velocities
$\tilde{v}_2, \tilde{v}_{12}, \tilde{v}_{12}^0$	(29), (A8), (57)	(Complex) resonant velocities
α, β	(5)	Rabi frequencies
γ_{ij}	(6)	Relaxation rate of σ_{ij}
$\gamma_B, \gamma_N, \gamma_B^0, \gamma_N^0$	(36), (37), (50), (51)	Effective decay rates
$\gamma(\epsilon)$	(39)	Resonance linewidth
$\bar{\gamma}, \Gamma, \Gamma'$	(42d), (42a), (42e)	Effective decay rates
$\delta_1, \delta_2, \delta_{12}$	(A3)	Frequency detunings
$\delta(\epsilon)$	(34)	Probe frequency detuning
$\Delta, \Delta', \Delta_2$	(42a), (42e), (72)	Frequency detunings
Δg	(28b)	Gain change
Δn_1	(85)	Population change
$\Delta\sigma_{01}^{(1)}, \Delta\sigma_{11}^{(2)}$	(23), (83)	Density matrix changes
$\zeta(\epsilon)$	(92), (93)	Population-change line shape
κ	(42c)	$(k_2 - k_1)/k_2$
Λ	(41b)	
$\xi(\epsilon)$	(53), (55)	Gain-change line shape
ρ_{ij}, σ_{ij}	(2)	Density matrix
χ	(A4)	$(\epsilon k_2 - k_1)/k_1$
ω_1, ω_2		Molecular frequencies
Ω_1, Ω_2	(1)	Laser frequencies
$\Omega_1^{(\epsilon)}$	(35)	Probe peak frequency

II. EQUATIONS OF MOTION

A. Background

When an intense monochromatic field E_2, frequency Ω_2, resonantly interacts with one of the transitions, 0-2, of a Doppler-broadened molecular (or atomic) gas, the level populations of the transition are altered over a narrow range of axial velocities centered about velocity v_2 satisfying the resonance condition (in the molecular rest frame) $\Omega_2 - k_2 v_2 = \omega_2$ (ω_2 being the molecular center frequency; $k_2 = \Omega_2/c$). This selective saturation of the level populations alters the spectral properties of a second coupled transition, 0-1, molecular center frequency ω_1, formed by either of the saturated levels and a third level (Fig. 3). In particular, if a weak monochromatic probe field E_1, frequency Ω_1, propagating either parallel (+) or antiparallel (−) to E_2 is tuned through the 0-1 transition, a narrow resonant change in transmission occurs, superimposed upon the broad Doppler profile, when Ω_1 is such that the probe field interacts with molecules of velocity v_2: $\Omega_1 = \omega_1 \pm k_1 v_2$ ($k_1 = \Omega_1/c$). This effect, called laser-induced line narrowing, has been the subject of numerous theoretical[4] and experimental[5] investigations devoted to studying the line shape of the change signal and using the narrow resonances thus obtained in high-resolution spectroscopic studies.[6] It is now well known that this effect cannot be analyzed in terms of population-saturation considerations alone, and that coherent processes play an important role. For example, via double-quantum processes a molecule initially in level 2 can undergo transition to level 1 by exchanging two photons of energy $\hbar\Omega_1$ and $\hbar\Omega_2$ with the applied radiation fields without loss of phase memory.

Because of the close correspondence with the Raman effect, transitions of this kind are sometimes called Raman-type processes.[22] Such processes exhibit very different dependence on molecular velocity, according to whether E_1 and E_2 are co-propagating or counter-propagating. This difference gives rise to a directional anisotropy in the net response, comprised of contributions from molecules of all velocities. Thus, the line shapes observed in co-propagating case (forward change signal) and counter-propagating case (backward change signal) always differ, in some cases dramatically. This directional anisotropy has been used to advantage in the recently introduced high-resolution spectroscopic techniques using Doppler-free two-photon absorption.[23]

The aim of this paper is to study the transient response of the molecular medium as observed on the transmission of the probe field after E_2 is abruptly terminated. As will be seen, many of the features discussed in the introduction will occur. One particularly interesting feature lies in the relative time evolution of population-saturation contributions versus Raman-type processes. As soon as E_2 is terminated Raman-type processes cease to occur, since E_2 is absent and can have no direct influence. However, the initial (steady-state) value of $P_1(t)$, the optical polarization oscillating at Ω_1, is influenced by the Raman-type processes occuring during the preparative step ($t \leq 0$). The probe change signals are completely determined by $P_1(t)$. Therefore, as $P_1(0)$ decays the directional anisotropy and other features of the change-signal line shapes associated with Raman-type processes will gradually disappear. This effect is particularly striking when the polarization decay rate ("T_2 processes") exceeds that of the level populations ("T_1 processes"), $T_2 \ll T_1$, so that the change signals can persist well beyond the decay of $P_1(0)$. In this case the shape of the forward change signal will evolve in time, as the influence of Raman-type processes decreases, and with increasing time delay the initially different forward and backward change-signal line shapes will eventually become identical. This opens the possibility of uniquely distinguishing the influence of Raman-type processes from that of population saturation and to separately measure the associated decay rates.

B. Coupled equations in the slowly varying envelope approximation

Consider a sample cell of gas molecules irradiated by two e.m. fields, $E_1(\Omega_1)$ and $E_2(\Omega_2)$, propagating along the z axis, having wave vectors k_1 and ϵk_2, $\epsilon = +1$ or -1 according to whether E_2 propagates parallel or antiparallel to E_1:

$$E_1 = \mathcal{E}_1^0 \cos(\Omega_1 t - k_1 z), \qquad E_2 = \mathcal{E}_2^0 \cos(\Omega_2 t - \epsilon k_2 z). \tag{1}$$

The molecular energy levels of interest, levels 0, 1, and 2, form a pair of Doppler-broadened transitions with molecular center frequencies ω_1 and ω_2 sharing a common level (Fig. 3). It is assumed that Ω_1 is close to ω_1 and Ω_2 to ω_2, so that E_j resonates with the 0-j transition ($|\Omega_j - \omega_j| <$ Doppler width). It is further assumed that E_2 cannot resonate with the 0-1 transition, nor E_1 with the 0-2 transition. This can be ensured either by proper choice of the polarizations of the E fields or by having the molecular center frequencies sufficiently separated ($|\omega_1 - \omega_2| >$ Doppler widths). To be specific, the problem will be formulated for the three-level configuration of Fig. 3(a), a folded system with level 0 lying lowest. The equations describing the other level configurations, Figs.

3(b) and 3(c), are more or less the same.[24(a)]

The system's time evolution can be conveniently described by means of the ensemble-averaged density-matrix formalism, in which $\rho_{ij}(v)$ is the density-matrix element describing the molecules with axial (z-axis) velocity component v. ρ_{jj} is the population of level j, $\rho_{0j}(j=1,2)$ is the optical coherence associated with the 0-j transition (it is proportional to the induced polarization oscillating at Ω_j), and ρ_{12} represents the macroscopic molecular coherence induced between levels 1 and 2. The following transformation allows one to go into the rotating frame:

$$\begin{aligned}
&\rho_{ii}=\sigma_{ii}\,,\\
&\rho_{01}=\sigma_{01}\exp\left[i(\Omega_1 t-k_1 z)\right],\\
&\rho_{02}=\sigma_{02}\exp\left[i(\Omega_2 t-\epsilon k_2 z)\right],\\
&\rho_{12}=\sigma_{12}\exp\left\{i\left[(\Omega_2-\Omega_1)t-(\epsilon k_2-k_1)z\right]\right\},
\end{aligned}\tag{2}$$

where the σ_{ij} are the slowly varying envelopes ($\partial\sigma_{ij}/\partial t \ll \omega\sigma_{ij}$, $\partial\sigma_{ij}/\partial z \ll k\sigma_{ij}$). In the rotating-wave approximation the σ_{ij} obey the following equations of motion[24b]:

$$\begin{aligned}
&\dot{\sigma}_{00}+\gamma_0(\sigma_{00}-n_0)=-\tfrac{1}{2}i\alpha(\sigma_{01}-\sigma_{01}^*)-\tfrac{1}{2}i\beta(\sigma_{02}-\sigma_{02}^*)\,,\\
&\dot{\sigma}_{11}+\gamma_1(\sigma_{11}-n_1)=\tfrac{1}{2}i\alpha(\sigma_{01}-\sigma_{01}^*)\,,\\
&\dot{\sigma}_{22}+\gamma_2(\sigma_{22}-n_2)=\tfrac{1}{2}i\beta(\sigma_{02}-\sigma_{02}^*)\,,\\
&\dot{\sigma}_{12}+L_{12}^*\sigma_{12}=\tfrac{1}{2}i\alpha\sigma_{02}-\tfrac{1}{2}i\beta\sigma_{01}^*\,,\\
&\dot{\sigma}_{01}+L_1\sigma_{01}=\tfrac{1}{2}i\alpha(\sigma_{11}-\sigma_{00})+\tfrac{1}{2}i\beta\sigma_{12}^*\,,\\
&\dot{\sigma}_{02}+L_2\sigma_{02}=\tfrac{1}{2}i\beta(\sigma_{22}-\sigma_{00})+\tfrac{1}{2}i\alpha\sigma_{12}\,,
\end{aligned}\tag{3}$$

where $\dot{\sigma}=d\sigma/dt$,

$$\begin{aligned}
&L_1=\gamma_{01}+i(\Omega_1-\omega_1-k_1 v)\,,\\
&L_2=\gamma_{02}+i(\Omega_2-\omega_2-\epsilon k_2 v)\,,\\
&L_{12}=\gamma_{12}+i[\Omega_1-\Omega_2-\omega_1+\omega_2-(k_1-\epsilon k_2)v]\,,
\end{aligned}\tag{4}$$

and

$$\alpha=\mu_{01}\mathcal{E}_1^0/\hbar\,,\quad \beta=\mu_{02}\mathcal{E}_2^0/\hbar\,.\tag{5}$$

In Eqs. (3)–(5), μ_{0j} is the dipole-moment matrix element connecting levels 0 and j. The Rabi frequencies α and β can be taken to be real without loss of generality. The background population density of level j (i.e., its population in the absence of the applied laser field) in the narrow interval between v and $v+dv$ is denoted by $n_j(v)dv$,

$$n_j(v)=\bar{n}_j G(v)\,,\quad \int G(v)\,dv=1\,,$$

where $\bar{n}_j$ is the total background population density of level j and $G(v)$ is the normalized velocity distribution. Finally, γ_i and γ_{ij} are the decay rates of the population of level i and the σ_{ij} coherence respectively. In general,

$$\gamma_{ij}\geq\tfrac{1}{2}(\gamma_i+\gamma_j)\,.\tag{6}$$

The equality in Eq. (6) holds only when phase-changing collisions are absent, for instance in the case of radiative decay or relaxation by inelastic collisions.

The macroscopic polarization associated with the 0-j transition is given by

$$P_j=\mathrm{Re}\left\{\mathcal{P}_j\exp\left[i(\Omega_j t-k_j z)\right]\right\},$$

with

$$\mathcal{P}_j=2\mu_{0j}\langle\sigma_{0j}\rangle\,,$$

where $\langle\ \rangle$ denotes velocity integration over $G(v)$. The net field associated with the 0-1 transition is composed of incident and reradiated components,

$$E_1(z,t)=\mathrm{Re}\left\{(\mathcal{E}_1^0+\Delta\mathcal{E}_1)\exp\left[i(\Omega_1 t-k_1 z)\right]\right\}.\tag{7}$$

In the experiments of interest the sample is assumed to be optically thin and short (no phase-matching problem[15]). In this case the amplitude of the reradiated field will be small compared to the incident field ($|\Delta\mathcal{E}_1|\ll\mathcal{E}_1^0$). At the output face of the sample cell ($z=l$), ΔE_1 is then given by[15]

$$\Delta\mathcal{E}_1=\frac{-2\pi i\Omega_1 l}{c}\,\mathcal{P}_1=\frac{-4\pi i\Omega_1 l}{c}\,\mu_{01}\langle\sigma_{01}\rangle\,.\tag{8}$$

This gives rise to a change in transmitted intensity at the probe frequency:

$$I_1(t)=I_1^0+\hbar\Omega_1\alpha l\,\mathrm{Im}\langle\sigma_{01}(t)\rangle\,,\tag{9a}$$

with $I_1=c|\mathcal{E}_1|^2/8\pi$ and I_1^0 the incident intensity of the probe field. The last term of this expression is the heterodyne beat between the incident probe field and the reradiated field. It will exhibit transient behavior when the saturating field is turned on or off.

The gain at the probe transition can be defined by

$$I_1(t)=I_1^0+gI_1^0\,.$$

We then have

$$g(t)=(8\pi/c)\Omega_1 l\mu_{01}\,\mathrm{Im}\langle\sigma_{01}\rangle/\mathcal{E}_1^0\,.\tag{9b}$$

In transmission studies, and also in studies of spontaneous emission line shapes at the 0-1 transition,[4] g is the quantity of experimental interest.

In some experiments[23] it may be more convenient to detect the net fluorescence emitted from a transition formed by level 1 and another lower-lying level, level 4, as E_1 is tuned through the 0-1 transition. In this case the net intensity emitted at the 1-4 transition, frequency ω, into solid angle $d\Omega$ is given by[25,26]

$$I_F=(\omega^4 d\Omega/2\pi c^3)\mu_{14}^2\langle\sigma_{11}\rangle\,,\tag{10}$$

where μ_{14} is the 1-4 transition matrix element.

Note that in experiments of this type one directly monitors the time evolution of the total population of level 1, as opposed to the transmission experiments, which study $\langle\sigma_{01}\rangle$. However, the transient signals observed in the two cases will be similar, since the two quantities are intimately related.

C. General way of solving the equations

When the condition $\alpha \ll \gamma_{ij}$ is fulfilled, the probe field is weak enough so that Eqs. (3) can be solved by using a perturbation expansion of σ_{ij} in α:

$$\sigma_{ij} = \sum_n \sigma_{ij}^{(n)} ,$$

where $\sigma_{ij}^{(n)}$ is proportional to α^n. This expansion of σ_{ij}, when inserted in Eqs. (3), leads to a set of equations which can be solved for arbitrary intensities of the saturating field, i.e., for arbitrary values of β.

The zeroth-order set of equations corresponds to the case in which the probe field is absent ($\alpha = 0$). In this case the molecular system becomes equivalent to a two-level system:

$$\dot{\sigma}_{00}^{(0)} + \gamma_0(\sigma_{00}^{(0)} - n_0) = -\tfrac{1}{2} i\beta(\sigma_{02}^{(0)} - \sigma_{02}^{(0)*}) , \tag{11a}$$

$$\dot{\sigma}_{22}^{(0)} + \gamma_2(\sigma_{22}^{(0)} - n_2) = \tfrac{1}{2} i\beta(\sigma_{02}^{(0)} - \sigma_{02}^{(0)*}) , \tag{11b}$$

$$\dot{\sigma}_{02}^{(0)} + L_2\sigma_{02}^{(0)} = \tfrac{1}{2} i\beta(\sigma_{22}^{(0)} - \sigma_{00}^{(0)}) . \tag{11c}$$

There is no coherence between level 1 and levels 0-2,

$$\sigma_{01}^{(0)}(t) = \sigma_{12}^{(0)}(t) = 0 , \tag{12}$$

and the population of level 1 is given by its background value,

$$\sigma_{11}^{(0)}(t) = n_1 . \tag{13}$$

In the first order in α the E_1 field does not change the level populations, nor the 0-2 optical polarization,

$$\sigma_{ii}^{(1)}(t) = \sigma_{02}^{(1)}(t) = 0 , \tag{14}$$

but it induces an optical polarization at the 0-1 transition, as well as a coherence between levels 1 and 2. These two quantities satisfy the coupled equations

$$\dot{\sigma}_{01}^{(1)} + L_1\sigma_{01}^{(1)} = \tfrac{1}{2} i\alpha(n_1 - \sigma_{00}^{(0)}) + \tfrac{1}{2} i\beta\sigma_{12}^{(1)*} , \tag{15a}$$

$$\dot{\sigma}_{12}^{(1)*} + L_{12}\sigma_{12}^{(1)*} = -\tfrac{1}{2} i\alpha\sigma_{02}^{(0)*} + \tfrac{1}{2} i\beta\sigma_{01}^{(1)} . \tag{15b}$$

The 1-2 coherence results from Raman-type processes in which for example, the molecules undergo transitions from levels 2 to 1 by emitting a photon at Ω_2 and absorbing a photon at Ω_1.[22]

In the case of fluorescence measurements one needs to solve the equations up to the second order in α. The E_1-induced population change of level 1 is given by

$$\dot{\sigma}_{11}^{(2)} + \gamma_1\sigma_{11}^{(2)} = \tfrac{1}{2} i\alpha(\sigma_{01}^{(1)} - \sigma_{01}^{(1)*}) . \tag{16}$$

As can be seen from Eq. (16), in the *steady-state regime* fluorescence techniques and transmission measurements give equivalent information, since $\gamma_1\sigma_{11}^{(2)} = -\alpha\,\mathrm{Im}\sigma_{01}^{(1)}$. This is a direct consequence of the energy conservation condition at the 0-1 transition.

Note that Eqs. (11)–(16) are valid regardless of the form of the time variations of β. In the following we shall deal with the free-decay case (constant $\beta \neq 0$ for $t < 0$, $\beta = 0$ for $t \geq 0$).

III. CALCULATION OF THE PROBE FIELD GAIN

A. Response of a molecular velocity group

In the steady-state regime ($t \leq 0, \dot{\sigma} = 0$), the solution of the zeroth-order Eqs. (11) is given by

$$\sigma_{02}^{(0)*}(0) = -i\,\frac{n_{20}\beta}{2}\,\frac{L_2}{|L_2(\beta)|^2} , \tag{17a}$$

$$\sigma_{00}^{(0)}(0) = n_0 + \frac{\beta^2}{2}\,\frac{\gamma_{02}}{\gamma_0}\,\frac{n_{20}}{|L_2(\beta)|^2} , \tag{17b}$$

where

$$L_2(\beta) = \gamma_{02}(1+s)^{1/2} + i(\Omega_2 - \omega_2 - \epsilon k_2 v) , \tag{18}$$

the saturation parameter s is proportional to the intensity of the E_2 field,

$$s = \beta^2(\gamma_0 + \gamma_2)(2\gamma_0\gamma_2\gamma_{02})^{-1} , \tag{19}$$

and n_{j0} is the 0-j background inversion density,

$$n_{j0} = n_j - n_0 . \tag{20}$$

For $t > 0$ ($\beta = 0$) the decay of the population and of the 0-2 macroscopic polarization are straightforwardly given by

$$\sigma_{02}^{(0)*}(t) = \sigma_{02}^{(0)*}(0)e^{-L_2^* t} , \tag{21a}$$

$$\sigma_{00}^{(0)}(t) = n_0 + [\sigma_{00}^{(0)}(0) - n_0]e^{-\gamma_0 t} . \tag{21b}$$

The polarization at the probe frequency is obtained by solving Eqs. (15a) and (15b). The origin of the distinct contributions arising from population-saturation effects and Raman-type processes can be readily seen in the steady-state form of Eq. (15a),

$$L_1\sigma_{01}^{(1)} = \tfrac{1}{2} i\alpha(n_1 - \sigma_{00}^{(0)}) + \tfrac{1}{2} i\beta\sigma_{12}^{(1)*} . \tag{22}$$

The two terms on the right-hand side act as source terms to drive σ_{01}. The coupling between σ_{01} and the level populations is evident in the first term, which gives rise to the population-saturation contributions ("stepwise" transitions). The coupling of σ_{12} to the probe polarization appears in the second term, and is responsible for the occurrence of Raman-type contributions.

The expression for the polarization at the probe

frequency follows from Eqs. (15a) and (15b). It may be written in the form

$$\sigma_{01}^{(1)}(t) = \tfrac{1}{2} i\alpha \frac{n_{10}}{L_1} + \Delta\sigma_{01}^{(1)}(t) . \tag{23}$$

The first term on the right-hand side describes the linear response of the probe field. It is independent of β and so does not exhibit transient behavior. After velocity integration it gives rise to the constant Doppler-broadened background gain.

The second term of Eq. (23) describes the influence of the saturating field on the probe polarization. Its value in the steady state may be obtained from the simultaneous solution of Eqs. (15a) and (15b) for $\dot{\sigma}_{ij} = 0$,

$$\Delta\sigma_{01}^{(1)}(0) = \frac{-\frac{1}{8} i\alpha\beta^2}{L_1 L_{12} + \frac{1}{4}\beta^2} \left[\frac{n_{10}}{L_1} + \frac{n_{20}}{|L_2(\beta)|^2} \times \left(L_2 + 2\,\frac{\gamma_{02}}{\gamma_0} L_{12} \right) \right] . \tag{24}$$

The transient evolution of $\Delta\sigma_{01}^{(1)}$ is determined by Eq. (15a) with β set equal to zero. This leads to

$$\Delta\dot{\sigma}_{01}^{(1)} + L_1 \Delta\sigma_{01}^{(1)} = \tfrac{1}{2} i\alpha (n_0 - \sigma_{00}^{(0)}) . \tag{25}$$

The solution is obtained with the help of Eqs. (17) and (21),

$$\Delta\sigma_{01}^{(1)}(t) = \Delta\sigma_{01}^{(1)}(0) e^{-L_1 t} + i\,\frac{\alpha\beta^2}{4}\,\frac{\gamma_{02}}{\gamma_0}\,\frac{n_{20}}{|L_2(\beta)|^2}\,\frac{e^{-L_1 t} - e^{-\gamma_0 t}}{L_1 - \gamma_0} , \tag{26}$$

where $\Delta\sigma_{01}^{(1)}(0)$ is given by Eq. (24). The first term in Eq. (26) represents the decay of the polarization created before $t = 0$. The second term comes from the coupling between population and polarization, which still exists after $t = 0$. Since the reradiated field is proportional to $\Delta\sigma_{01}(t) e^{i\Omega_1 t}$ [see Eqs. (7), (8)] the decay of $\Delta\sigma_{01}^{(1)}$ ($e^{-L_1 t}$ term) gives rise to emission of radiation at the Doppler-shifted natural frequency, $\omega_1 + k_1 v$, while the change in the population of level 0 ($e^{-\gamma_0 t}$ term) modifies the stimulated emission at the probe frequency, Ω_1. Also note that since E_2 is absent after $t = 0$, $\sigma_{01}^{(1)}$ is not coupled to $\sigma_{12}^{(1)}$, and so transient Raman processes do not show up (as they would in optical nutation). However, Raman-type processes do manifest themselves in the steady-state polarization, $\Delta\sigma_{01}^{(1)}(0)$, and so their influence decays with the characteristic decay time of the 0-1 polarization.

B. Velocity integrated gain

To obtain the expression for the probe gain [Eq. (9b)], one must average the 0-1 polarization over the molecular velocity distribution. In the following, a Gaussian distribution,

$$G(v) = (1/u\sqrt{\pi}) e^{-v^2/u^2} , \tag{27}$$

will be used, with u the thermal velocity. Using Eqs. (9b) and (23), one finds that the gain at the probe transition is given by

$$g = g_0 + (8\pi k_1 l \mu_{01}^2/\hbar\alpha)\,\mathrm{Im}\langle \Delta\sigma_{01}^{(1)}(v, t)\rangle , \tag{28a}$$

with g_0 the linear background gain. In the Doppler-broadened limit ($\gamma_{01} \ll k_1 u$)

$$g_0 = 4\pi l \mu_{01}^2 N_{10}/\hbar ,$$

with

$$N_{10} = \pi \bar{n}_{10} G(v_1) , \quad v_1 = (\Omega_1 - \omega_1)/k_1 .$$

The probe field change signal may then be defined as

$$\Delta g(t) = (2k_1 g_0/\alpha N_{10})\,\mathrm{Im}\langle \Delta\sigma_{01}^{(1)}(v, t)\rangle . \tag{28b}$$

In the fully Doppler-broadened limit, where the natural widths, γ_{ij}, and the power-broadened 0-2 transition linewidth, $\gamma_{02}(1+s)^{1/2}$, are much smaller than the Doppler widths $k_1 u$ and $k_2 u$, $G(v)$ is slowly varying compared to $\Delta\sigma(v, t)$ [Eq. (26)] and can be taken as constant in the velocity integration. This integration can then be performed using contour integration, by considering $\Delta\sigma$ as an analytic function of the complex variable $\tilde{v}$. The path of integration is the real axis of the complex plane, and the contour can be closed at $+\infty$ and $-\infty$ in the upper half of the complex plane in order that the exponential term $e^{ik_1\tilde{v}t}$ (coming from $e^{-L_1 t}$) vanishes for infinite values of the imaginary part of $\tilde{v}$, at $t > 0$. The integration then consists of evaluating $\Delta\sigma(v, t)$ at the poles lying in the upper half of the complex plane.[27]

In $\Delta\sigma_{01}^{(1)}(v, t)$ the poles corresponding to $L_1 = 0$ and $L_1 - \gamma_0 = 0$ lie in the lower half of the complex plane and do not contribute. Of the two poles coming from $|L_2(\beta)|^2 = 0$, only one brings a nonvanishing contribution. The denominator $(L_1 L_{12} + \frac{1}{4}\beta^2)^{-1}$ is much more complicated: its two poles are analyzed in Appendix A. When $k_1 - \epsilon k_2 \geq 0$, there is no contribution. This condition corresponds to either $\epsilon = -1$ (counter-propagating waves), or $\epsilon = +1$ and $k_1 \geq k_2$. In the remaining case ($\epsilon = 1$; $k_2 > k_1$) one of the poles lies in the upper half of the complex plane and brings an additional contribution to $\langle \Delta\sigma \rangle$.[24(a)]

1. $k_1 - \epsilon k_2 \geq 0$

As an example of the velocity integration, we shall discuss this first case in some detail. The pole of $|L_2(\beta)|^{-2}$ lying in the upper half of the complex plane is given by

$$k_2 \tilde{v}_2 = \epsilon(\Omega_2 - \omega_2) + i\gamma_{02} Q , \tag{29}$$

where

$$Q=(1+s)^{1/2}. \tag{30}$$

Using the residue theorem, this pole leads to the following expression for the probe field change signal:

$$\Delta g(\tilde{v}_2,t,\epsilon)=-g_0\left(\frac{k_1}{2k_2}\frac{\beta^2}{\gamma_0^2 Q}\frac{N_{20}}{N_{10}}\right)\mathrm{Re}\gamma_0\left[\frac{e^{-\gamma_0 t}-e^{-[\gamma_B+i\delta(\epsilon)]t}}{\gamma_B-\gamma_0+i\delta(\epsilon)}+\frac{\gamma_N+\frac{1}{2}\gamma_0(1+\epsilon Q)+i\delta(\epsilon)}{[\gamma_B+i\delta(\epsilon)][\gamma_N+i\delta(\epsilon)]+\frac{1}{4}\beta^2}\,e^{-[\gamma_B+i\delta(\epsilon)]t}\right], \tag{31}$$

where N_{20} is proportional to the 0-2 inversion density for the resonant molecular velocity v_2,

$$N_{20}=\pi\bar{n}_{20}G(v_2), \tag{32}$$

$$v_2=\epsilon(\Omega_2-\omega_2)k_2^{-1}, \tag{33}$$

and $\delta(\epsilon)$ is the detuning of the probe frequency from the line center of the steady-state saturation resonance, $\Omega_1^{(\epsilon)}$,

$$\delta(\epsilon)=\Omega_1-\Omega_1^{(\epsilon)}, \tag{34}$$

$$\Omega_1^{(\epsilon)}=\omega_1+\epsilon(k_1/k_2)(\Omega_2-\omega_2). \tag{35}$$

Finally, two effective decay rates have been introduced,

$$\gamma_B=\gamma_{01}+(k_1/k_2)\gamma_{02}Q, \tag{36}$$

$$\gamma_N=\gamma_{12}+[(k_1-\epsilon k_2)/k_2]\gamma_{02}Q. \tag{37}$$

The physical interpretation of Eq. (31) is as follows: (i) The last term in brackets describes the decay of the initial polarization induced by the saturating field E_2 before $t=0$. Since this polarization is due to molecules in the velocity band centered at v_2, the decay occurs at the Doppler-shifted frequency $\omega_1+k_1v_2=\Omega_1^{(\epsilon)}$. The corresponding emitted field interferes with the probe field to give a beat at frequency $\delta(\epsilon)$. The decay of this beat consists of two contributions: the γ_{01} term, which is due to the decay of the 0-1 polarization, and a "Doppler dephasing" contribution, $\gamma_{02}Qk_1/k_2$, which is due to the velocity spread of the excited molecules [$\mathrm{Im}\,\tilde{v}_2$ in Eq. (29)] and gives rise to a corresponding spread in the emitted frequencies, leading to destructive interference in a time of the order of $k_2(k_1\gamma_{02}Q)^{-1}$. Notice that the latter contribution contains the influence of power broadening in the preparative step. Finally, as expected, for $t=0$, the last term of Eq. (31) gives rise to the well-known line shape of the saturation resonance in a three-level system.[4]

(ii) The first term in brackets is a pure transient contribution (it cancels for both $t=0$ and $t\gg\gamma^{-1}$), coming from the coupling of the 0-1 polarization to the transient population of level 0. Since this term describes the change in stimulated emission resulting from population decay, it contains a contribution ($e^{-\gamma_0 t}$) exhibiting neither Doppler dephasing (hence no dephasing due to power broadening), nor beat frequency.

When there are no dephasing collisions [$\gamma_{ij}=\frac{1}{2}(\gamma_i+\gamma_j)$], Eq. (31) may be simplified to yield

$$\Delta g(\tilde{v}_2,t,\epsilon)=-g_0\left(\frac{k_1}{2k_2}\frac{\beta^2}{\gamma_0^2 Q}\frac{N_{20}}{N_{10}}\right)\mathrm{Re}\,\frac{\gamma_0^2}{\gamma_B-\gamma_0+i\delta(\epsilon)}\times\left(\frac{e^{-\gamma_0 t}}{\gamma_0}-\frac{1-\epsilon Q}{2}\frac{e^{-[\gamma_B+i\delta(\epsilon)]t}}{\gamma(\epsilon)+i\delta(\epsilon)}\right), \tag{38}$$

where $\gamma(\epsilon)$ is the width of the Lorentzian line shape observed in the steady-state regime ($t=0$),

$$\gamma(\epsilon)=\tfrac{1}{2}\gamma_1+(k_1/k_2)\gamma_{02}Q-\epsilon(\gamma_0/2)Q. \tag{39}$$

Equation (39) straightforwardly shows the well-known result that the change-signal linewidth is narrower for forward scattering ($\epsilon=+1$) than for backward scattering ($\epsilon=-1$). Since the net areas under the gain curves are equal,[26] it follows that the peak amplitude of the forward signal is larger than that of the backward signal. This point and others will be discussed in more detail in the following section.

2. $\epsilon=+1;\ k_2>k_1$

In the case of forward scattering with $k_2>k_1$ [Ref. 24a] there is an additional contribution to the change-signal gain, coming from the new resonant velocity $\tilde{v}_{12}=x_-(\beta)/k_1$, where $x_-(\beta)$ is defined in Eq. (A8). We then have

$$\Delta g(t,+)=\Delta g(\tilde{v}_2,t,+)+\Delta g(\tilde{v}_{12},t,+), \tag{40}$$

where $\Delta g(\tilde{v}_2,t,+)$ is given by Eq. (31), and

$$\Delta g(\tilde{v}_{12},t,+)=-\tfrac{1}{2}g_0S^2\,\mathrm{Re}\,\frac{e^{-(\Gamma'+i\Delta')t/\kappa}}{(\Gamma+i\Delta)\Lambda}, \tag{41a}$$

with

$$\Lambda^{-1}=\frac{1}{\Gamma'+i\Delta'}+\frac{k_2}{k_1}\frac{N_{20}}{N_{10}}\frac{[\Gamma'-\kappa\gamma_{01}+i(\Delta'-\kappa\delta)]+\kappa(\gamma_{02}/\gamma_0)[(k_1/k_2)\gamma_0+\bar{\gamma}-\Gamma+i(\delta-\Delta)]}{\kappa^2\gamma_{02}^2Q^2-(k_2/k_1)^2[\Gamma'-\kappa\gamma_{01}+i(\Delta'-\kappa\delta)]^2}. \tag{41b}$$

In this equation the following notation is used:

$$\Gamma + i\Delta = [(\bar{\gamma} + i\delta)^2 + S^2]^{1/2}, \tag{42a}$$

$$S = \beta[(k_1/k_2)\kappa]^{1/2}, \tag{42b}$$

$$\kappa = (k_2 - k_1)/k_2, \tag{42c}$$

$$\bar{\gamma} = (k_1/k_2)\gamma_{12} + \kappa\gamma_{01}, \tag{42d}$$

$$\Gamma' = \tfrac{1}{2}(\Gamma + \bar{\gamma}), \quad \Delta' = \tfrac{1}{2}(\Delta + \delta). \tag{42e}$$

with δ the probe frequency detuning [Eq. (34) with $\epsilon = +1$]. The sign of the complex square root in Eq. (42a) is determined by continuity from $\bar{\gamma} + i\delta$ at $\beta = 0$. The physical interpretation of Eq. (41) is not as simple as that of Eq. (31), and will be elaborated on in the following sections. As shown below, the contribution from the v_{12} group arises from Raman-type processes. (For small β, $\bar{v}_{12}$ is determined by the resonance condition $L_{12} = 0$.) This is the reason why this contribution does not vanish even if the 0-2 transition is transparent to the saturating field ($N_{20} = 0$, $N_{10} \neq 0$). For high intensities we shall see that this contribution exhibits dynamic Stark splitting ["Autler-Townes effect"[28]]. Finally, note that $\Delta g(\bar{v}_{12}, t, +)$ simplifies considerably when there are no phase-changing collisions [$\gamma_{ij} = \frac{1}{2}(\gamma_i + \gamma_j)$] and

$$k_2 = 2k_1, \quad \gamma_0 = \gamma_2 .$$

The quantity Λ, Eq. (41b), then reduces to

$$\frac{1}{\Lambda} = \frac{1}{\Gamma' + i\Delta'} - \frac{N_{20}/N_{10}}{\frac{1}{2}\gamma_1 + i\delta} . \tag{43}$$

C. General features of the probe field gain

1. Equal-area property

A very interesting feature of the gain curves is that the area under the forward change signal is equal to that under the backward change signal at any time during the decay. Thus, it can be readily shown by contour integration of Eqs. (31) and (41) that

$$\int \Delta g(\bar{v}_2, t, \epsilon)\, d\delta(\epsilon) = -g_0 \frac{\pi k_1}{2k_1} \frac{\beta^2}{\gamma_0 Q} \frac{N_{20}}{N_{10}} e^{-\gamma_0 t}$$

and (44)

$$\int \Delta g(\bar{v}_{12}, t, +)\, d\delta = 0 .$$

We thus obtain the statement of the equal-area property,

$$\int \Delta g(t, +)\, d\delta(+) = \int \Delta g(t, -)\, d\delta(-) . \tag{45}$$

The equal area property of the steady-state change signals (i.e., at $t = 0$) has been discussed before.[29] The fact that the areas remain equal during the decay of the change signals follows from a general result presented in Ref. 26. According to this result, the time behavior of the frequency-integrated gain should follow the decay of $\langle \sigma_{00}(t) \rangle$, the velocity-integrated population of level 0. It is easily seen from Eqs. (17b) and (21b) that

$$\langle \sigma_{00}(t) \rangle = \bar{n}_0 + \frac{\beta^2}{2k_2\gamma_0 Q} N_{20} e^{-\gamma_0 t} .$$

Thus, using Eq. (44) we can write Eq. (45) in the form

$$\int \Delta g(t, \epsilon)\, d\delta(\epsilon) = -\frac{4\pi^2 k_1 \mu_{10}^2 l}{\hbar} (\langle \sigma_{00}(t) \rangle - \bar{n}_0), \tag{46}$$

in agreement with the general result.[30] It also follows from this result that the net area under the $\Delta g(\bar{v}_{12}, t, \epsilon)$ change signal is always zero. Thus, this quantity is either identically zero, as in the $\epsilon = -1$ case, or it exhibits sign changes as the detuning is varied, as in the $\epsilon = +1$ case.

Finally, it should be mentioned that these results hold for any particular velocity group, as can be seen from the frequency integration of Eqs. (24) and (26), which leads to a relation similar to Eq. (46). Thus, Eq. (46) is not restricted to the fully Doppler-broadened limit. It holds for a velocity distribution of arbitrary width, including the case of complete homogeneous broadening [$G(v)$ sharp].

The equal-area property will be made use of below in analyzing the frequency behavior of the change-signal curves.

2. Independent-field approximation (IFA)

The independent-field approximation (sometimes referred to as the rate-equation approximation) assumes that E_1 and E_2 interact independently with their respective transitions. The effects of Raman-type processes are neglected, and so coupling only occurs through saturation of the level populations. This limit can be obtained easily from Eqs. (31) and (41) by taking the limit $\gamma_{12} \to \infty$. As can be seen from Eqs. (3), this has the effect of completely destroying the influence of Raman-type processes. In the limit $\Delta g(\bar{v}_{12}, t, +)$ vanishes and one obtains

$$\Delta g_{\mathrm{IFA}}(t, \epsilon) = -g_0 \left(\frac{k_1}{2k_2} \frac{\beta^2}{\gamma_0^2 Q} \frac{N_{20}}{N_{10}} \right) \times \mathrm{Re} \left\{ \frac{\gamma_0^2}{\gamma_B - \gamma_0 + i\delta(\epsilon)} \times \left[\frac{e^{-\gamma_0 t}}{\gamma_0} - \frac{e^{-[\gamma_B + i\delta(\epsilon)]t}}{\gamma_B + i\delta(\epsilon)} \right] \right\}. \tag{47}$$

Therefore, in the IFA there is no directional anisotropy and forward and backward change signals are the same. For weak saturation the change

signals in the IFA limit are identical to that of the $\epsilon=-1$ case [see Eq. (53), below]. However, for $\beta \gg \gamma$ the saturation behavior of the IFA result differs from that of the $\epsilon=-1$ case. This is readily apparent in the case where there are no dephasing collisions, Eq. (38), since the factor $(\gamma_B+i\delta)^{-1}$ appears in the second term in square brackets in Eq. (47) instead of $\frac{1}{2}(1+Q)/[\gamma(-)+i\delta(-)]$. Thus, for $t \ll \gamma_B^{-1}$ the IFA predicts Lorentzian forward and backward change signals of width γ_B rather than $\gamma(\epsilon)$. However, for $\gamma_0^{-1} > t \gtrsim \gamma_B^{-1}$, when the initial polarization has decayed away, both forward and backward change signals evolve towards the IFA value (see discussion in Sec. V A).

IV. FEATURES OF THE WEAK FIELD RESPONSE

When the saturating field is not intense ($\beta \ll \gamma_{ij}$), the results can be simplified by expanding Eqs. (31) and (41) in orders of β/γ. At the second order we have

$$\Delta g(\bar{v}_2^0, t, \epsilon) = -g_0\left(\frac{k_1}{2k_2}\,\frac{\beta^2}{\gamma_0^2}\,\frac{N_{20}}{N_{10}}\right) \mathrm{Re}\,\gamma_0\left[\frac{\exp(-\gamma_0 t)-\exp\{-[\gamma_B^0+i\delta(\epsilon)]t\}}{\gamma_B^0-\gamma_0+i\delta(\epsilon)} + \frac{\gamma_N^0+\frac{1}{2}\gamma_0(1+\epsilon)+i\delta(\epsilon)}{[\gamma_B^0+i\delta(\epsilon)][\gamma_N^0+i\delta(\epsilon)]}\exp\{-[\gamma_B^0+i\delta(\epsilon)]t\}\right], \tag{48}$$

and

$$\Delta g(\bar{v}_{12}^0, t, +) = -g_0\left(\frac{k_1}{2k_2}\,\kappa\,\frac{\beta^2}{\gamma_0^2}\right) \mathrm{Re}\,\gamma_0^2\left(\frac{1}{\bar{\gamma}+i\delta}-\frac{N_{20}/N_{10}}{\gamma_{12}-\kappa\gamma_{02}+i\delta}\right)\frac{\exp[-(\bar{\gamma}+i\delta)t/\kappa]}{\bar{\gamma}+i\delta}\,. \tag{49}$$

In these equations γ_B^0 and γ_N^0 are the values taken by γ_B and γ_N for $\beta=0$,

$$\gamma_B^0 = \gamma_{01} + (k_1/k_2)\gamma_{02}\,, \tag{50}$$

$$\gamma_N^0 = \gamma_{12} + [(k_1-\epsilon k_2)/k_2]\gamma_{02}\,. \tag{51}$$

In obtaining Eq. (49), note that for $\beta/\gamma \ll 1$,

$$\Gamma + i\Delta = \Gamma' + i\Delta' = \bar{\gamma} + i\delta\,. \tag{52}$$

A. Counter-propagating waves

When the saturating and probe fields are propagating antiparallel to each other ($\epsilon=-1$), Δg has a simple form. The term in brackets in Eq. (48), which determines the line shape of the change signal, is equal to

$$\xi(-) = \frac{\exp(-\gamma_0 t)-\exp\{-[\gamma_B^0+i\delta(-)]t\}}{\gamma_B^0-\gamma_0+i\delta(-)} + \frac{\exp\{-[\gamma_B^0+i\delta(-)]t\}}{\gamma_B^0+i\delta(-)}\,. \tag{53}$$

The time-varying gain is proportional to the real part of $\xi(-)$. A first remarkable result is that this expression is independent of γ_{12}. This is related to the fact that for $\epsilon=-1$ the coupling of σ_{12} with σ_{01} cancels after velocity integration. When the two waves have opposite propagation directions, the Raman-type processes, responsible for the creation of the σ_{12} coherence, have a strong velocity dependence. When integrated over velocity their net effect vanishes.

At $t=0$, $\mathrm{Re}\,\xi(-)$ is a Lorentzian of width γ_B^0. If $\gamma_B^0 > \gamma_0$ then the $e^{-\gamma_B^0 t}$ terms will decay away in a time $\sim 1/\gamma_B^0$ leaving only the $e^{-\gamma_0 t}$ contribution, a Lorentzian of width $\gamma_B^0-\gamma_0$. As explained in Sec. III B 1, this term is induced by the decaying population of level 0. Its linewidth is narrower than that of the steady-state contribution because this term arises from a contribution to $\Delta\sigma_{01}^{(1)}$, driven by a decaying population transient [cf. Eq. (25)], thus causing narrowing. The narrowing of the $\xi(-)$ line shape in the time decay of the $\epsilon=-1$ change signal can be seen in Fig. 4(a).

If $\gamma_0 \geq \gamma_B^0$ the decaying change signal evolves in an entirely different way. The $e^{-\gamma_0 t}$ contribution decays rapidly, leaving the $e^{-\gamma_B^0 t}$ contributions, which oscillate at frequency $\delta(-)$. These terms are associated with free decay of the initial polarization. As explained earlier, the emitted radiation, which decays at the natural frequency of the prepared velocity group, $\omega_1 + k_1 v_2$, beats with the probe field

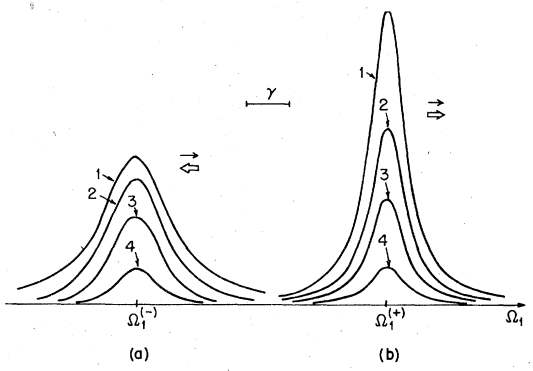

FIG. 4. Backward (a) and forward (b) change signals for weak saturation and no phase-changing collisions. The parameters are $k_1=k_2$, $N_{10}=N_{20}$, $\gamma_{ij}=\gamma$, and $\beta=0.1\gamma$. Time delays: $t_1=0$, $t_2=0.5/\gamma$, $t_3=1/\gamma$, and $t_4=2/\gamma$.

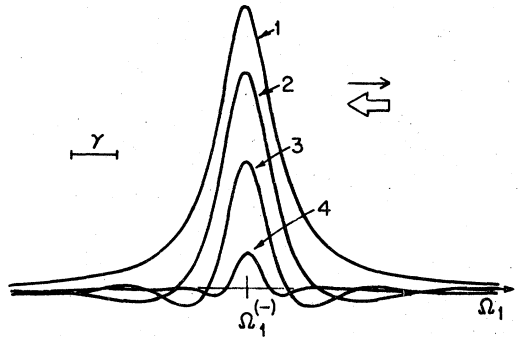

FIG. 5. Backward change signal for weak saturation and $\gamma_0 > \gamma_B^0$. The parameters are $k_1 = \frac{1}{2}k_2$, $\gamma_0 = \gamma$, $\gamma_1 = \gamma_2 = \frac{1}{10}\gamma$ (no phase-changing collisions), $\beta = 0.001\gamma$. Time delays: $t_1 = 0$, $t_2 = 1/\gamma$, $t_3 = 2/\gamma$, and $t_4 = 4/\gamma$.

to produce a gain component at $\delta(-)$. This type of beatnote is a characteristic feature of free-induction decay. Its counterpart in the frequency domain (at a fixed delay time) is a narrowing of the change-signal line shape accompanied by interference fringes. For example, the second term of Eq. (53) gives a line-shape contribution of the form

$$\frac{\gamma_B^0 \cos\delta t - \delta \sin\delta t}{(\gamma_B^0)^2 + \delta^2} \exp(-\gamma_B^0 t) \ . \tag{54}$$

This expression behaves like a Lorentzian for $t \ll 1/\gamma_B^0$, but for longer time delays it narrows and develops fringes of width $\delta \simeq \pi/t$. This narrowing occurs because, by observing change signals at delay times $\gtrsim (\gamma_B^0)^{-1}$ one is selecting molecules whose lifetimes are longer than the average, and whose linewidths are correspondingly narrower. Therefore, this method can be used to produce change signals much narrower than the natural widths, although in practice extreme line narrowing is limited by the intensity reduction occurring because of the decaying exponential factor $e^{-\gamma_B^0 t}$. Line shapes having similar physical origins have been exploited by Ramsey[31] in magnetic resonance experiments. Recently there have been several observations of this effect in the optical region.[32] The same type of line shape has been observed in time-delayed level crossing experiments.[33]

The actual line shape of Eq. (53) is composed of two such contributions, each of which exhibits fringes. It is plotted in Fig. 5 for $\gamma_B^0 = 0.825\gamma_0$, which corresponds to the case $k_1 = \frac{1}{2}k_2$ and $\gamma_1 = \gamma_2 = \frac{1}{10}\gamma_0$ [cf. Eq. (50)]. The observation of narrow resonances of this type opens interesting possibilities.

B. Co-propagating waves

For co-propagating fields the effect of Raman-type processes becomes important The term in brackets in Eq. (48) is equal to

$$\xi(+) = \frac{\exp(-\gamma_0 t)}{\gamma_B^0 - \gamma_0 + i\delta} + \frac{\gamma_0(\gamma_{01} + \gamma_{02} - \gamma_{12} - \gamma_0)\exp[-(\gamma_B^0 + i\delta)t]}{(\gamma_B^0 - \gamma_0 + i\delta)(\gamma_B^0 + i\delta)(\gamma_N^0 + i\delta)} \ . \tag{55}$$

The transient evolution of the gain line shape for $k_1 \geq k_2$ is proportional to $\mathrm{Re}\,\xi(+)$. As can be seen, Eq. (55) is a sensitive function of the presence of phase-changing collisions (see discussion below). When they are absent, $\gamma_{01} + \gamma_{02} = \gamma_{12} + \gamma_0$ [cf. discussion following Eq. (6)] and $\xi(+)$ reduces to

$$e^{-\gamma_0 t}/(\gamma_B^0 - \gamma_0 + i\delta) \ . \tag{56}$$

Thus, the contribution arising from the decay of the initial polarization completely cancels and the gain line shape decays as a simple exponential. The change signal remains Lorentzian throughout the decay, and Ramsey-type fringes are absent [Fig. 4(b)]. Note that in Eq. (56) the decay rate is completely governed by population relaxation and is independent of Doppler dephasing, in contrast to ordinary two-level free-induction decay.[7] By comparing Figs. 4(a) and 4(b) it can be seen that the areas of forward and backward change signals are equal at any given value of t, as expected.

For $k_2 > k_1$ there is an additional contribution to the change signal [cf. Eqs. (40) and (49)], entirely due to Raman-type processes. Indeed, when $k_2 \neq k_1$ the Raman-type processes are velocity dependent and can only occur for molecules in the $\tilde{v}_{12}^0$ velocity group, defined by the Raman resonance condition $L_{12}(v) = 0$

$$\tilde{v}_{12}^0 = (\Omega_2 - \Omega_1 - \omega_2 + \omega_1 + i\gamma_{12})/(k_2 - k_1) \ . \tag{57}$$

The real part of Eq. (57) is the statement of energy conservation for the Raman-type process in which a molecule undergoes a transition between levels 2 and 1 by emitting a photon Ω_2 and absorbing a photon Ω_1. The imaginary part of $\tilde{v}_{12}^0$ gives the width of the resonant velocity group. The decay of the v_{12}^0 velocity group after $t = 0$ leads to the $\Delta g(\tilde{v}_{12}^0, t, +)$ contribution. Since this contribution is associated with Raman-type processes, it can occur even if the molecular medium is transparent to the saturating field ($N_{20} = 0$). In this case the contribution given by Eq. (55) vanishes and the net change signal is proportional to the real part of

$$N_{10}(\bar{\gamma} + i\delta)^{-2} e^{-(\bar{\gamma} + i\delta)t/\kappa} \ . \tag{58}$$

The unusual time dependence of this expression can be understood by noting that the initial polar-

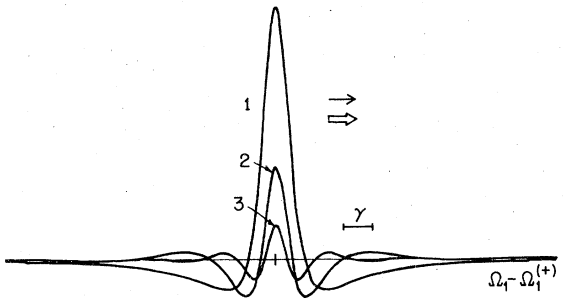

FIG. 6. Forward change signal, N_{10} contribution, for weak saturation. The parameters are $k_1=\frac{1}{2}k_2$, $\gamma_{ij}=\gamma$, and $\beta/\gamma=0.1$. Time delays: $t_1=0$, $t_2=0.5/\gamma$, and $t_3=1/\gamma$.

ization undergoes free decay according to $\exp[i(\omega_1+k_1\tilde{v}_{12}^0)t]\exp(-\gamma_{01}t)$. The resulting reradiated field then beats with E_1 to produce the time behavior of Eq. (58).

The time evolution of this change signal is plotted in Fig. 6. As can be seen, the change-signal area remains zero throughout the decay. Also note the development of Ramsey-type fringes as the decay progresses. The peculiar shape of this change signal has been experimentally verified by Hänsch *et al.*[34] in the steady-state regime.

C. Influence of phase-changing collisions

Phase-changing collisions strongly affect both the line shape and time evolution of the change signals. In the presence of phase-changing collisions the forward change signal is no longer given by the simple expression (56) and Doppler dephasing effects appear [see Eq. (55)]. In contrast, strong phase-interrupting collisions ($\gamma_B^0 \gg \gamma_0$) actually simplify the backward change signal, since Eq. (53) then reduces to $e^{-\gamma_0 t}(\gamma_B^0+i\delta)^{-1}$. Thus, in this limit the evolution of the change signal is completely determined by population decay processes. The contribution arising from the decaying polarization is negligible and Ramsey-type fringes are absent.

A case of special interest occurs when the transition frequencies are close ($\omega_1 \simeq \omega_2$) and the decay of the optical polarization is rapid compared to the other decay rates (fast T_2 processes):

$$\gamma_{02},\gamma_{01} \gg \gamma_0,\gamma_{12} \ . \tag{59}$$

In many atomic and molecular transitions these conditions can be achieved by using a linearly polarized saturating field and a probe field having a different polarization. In this case levels 1 and 2 are two magnetic sublevels of the same energy level and γ_{12} represents the relaxation rate of the coherence between them ("Zeeman coherence"),

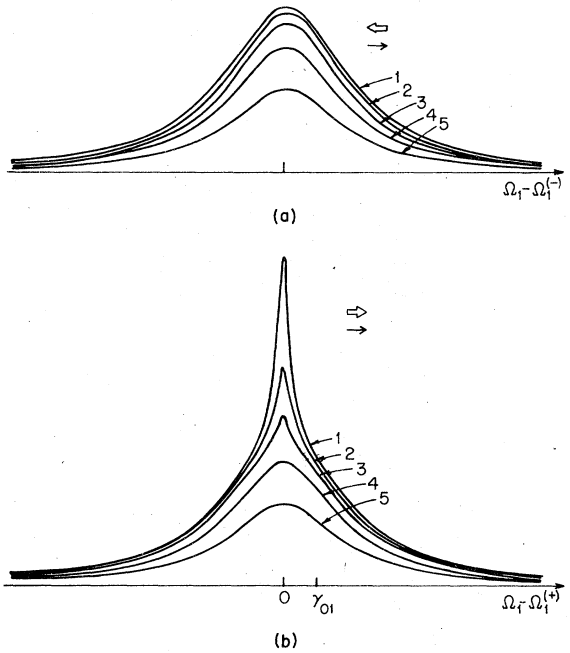

FIG. 7. Backward (a) and forward (b) change signals for strong phase-changing collisions and weak saturation. The parameters are $k_1=k_2$, $\gamma_0=\gamma_2=\gamma_{12}=\gamma$, $\gamma_{01}=\gamma_{02}=5\gamma$, and $\beta/\gamma=0.1$. Time delays: $t_1=0$, $t_2=0.5/\gamma_{01}$, $t_3=1/\gamma_{01}$, $t_4=2/\gamma_{01}$, and $t_5=4/\gamma_{01}$.

which is typically of the same order of magnitude as γ_0, the population decay rate, but much smaller than the decay rate of the induced optical polarization. When condition (59) is fulfilled $\xi(\epsilon)$ can be approximated by [cf. Eqs. (53) and (55)]

$$\xi(\epsilon)=\frac{\exp(-\gamma_0 t)}{\gamma_B^0+i\delta(\epsilon)}+\frac{1+\epsilon}{2}\,\frac{\gamma_0\exp(-\gamma_B^0 t)}{\gamma_B^0[\gamma_{12}+i\delta(\epsilon)]} \ . \tag{60}$$

The first term of Eq. (60) describes a broad resonance, width $\gamma_{01}+\gamma_{02}$, induced by the population saturation of level 0, which decays at characteristic rate γ_0. This is the only contribution to the backward decay [Fig. 7(a)]. However, in the forward direction there is an additional contribution [second term of Eq. (60)] in the form of a narrow resonance of width γ_{12}, induced by Raman-type processes [Fig. 7(b)]. This narrow contribution decays at a much faster rate, $\gamma_{01}+\gamma_{02}$, determined by the optical-polarization decay rate.

Steady-state (i.e., $t=0$) forward change signals exhibiting both broad and narrow features have been observed recently.[35] This type of line shape is very similar to the Zeeman-tuned saturation resonances observed in the intensity of the fluorescence emitted from a transition with degenerate magnetic sublevels resonating with a single-mode laser.[36] Such resonances, observed as a function of Zeeman tuning, consist of a narrow component,

associated with Zeeman coherence ("Hanle effect"), superimposed on a broader "population effect" resonance. These features are the counterparts of the Raman-type and population-saturation features, respectively, of Eq. (60), $\epsilon = +1$.[37]

The study of the transient behavior of the change signals in such a system provides a unique way of distinguishing population saturation and Raman-type processes, owing to their very different decay constants. A remarkable consequence of Eq. (60) is that after a time $\simeq (\gamma_{01}+\gamma_{02})^{-1}$ the narrow contribution decays away, and the forward change signal is reduced to a broad resonance identical to the backward signal. This type of behavior, in which a broad resonance decays slowly and a narrow resonance rapidly, is different from the usual frequency-time domain behavior of linear systems. It is a good example of the fact that in three-level free-decay frequency and time behavior are not connected in a simple way.

The results of recent experiments in which such behavior is observed in NH_3 will be reported elsewhere.[13]

V. SATURATION EFFECTS

When the intensity of the saturating field is large enough [saturation parameter $s \gtrsim 1$, Eq. (19)], new features appear including power broadening of the resonances, power dephasing of the decay rates and, in some cases, a new type of oscillatory behavior in the decaying change signals.

A. Power broadening and power dephasing

When $k_1 \geq \epsilon k_2$ (either counter-propagating waves or co-propagating waves with $k_1 > k_2$), the signal is given by $\Delta g(\tilde{v}_2, t, \epsilon)$, Eq. (31). As the intensity of the saturating field increases two features are noteworthy: (i) The change signals become power broadened and their amplitudes saturate; (ii) of the two decay rates, the one associated with population relaxation (γ_0) remains unchanged, while the one associated with polarization decay (γ_B) increases. This increase is due to power broadening of the velocity group excited during the preparative stage. The growing range of interacting molecular velocities increases the velocity ("Doppler") dephasing contribution to the relaxation rate. For large saturating intensities γ_B can exceed γ_0 by an order of magnitude, and the decaying change signal evolves in two distinct stages. For the sake of simplicity let us consider the case in which phase-changing collisions are absent, Eq (38).

(i) For $t \ll 1/\gamma_B$ the change signal is a Lorentzian of width $\gamma(\epsilon)$ [Eq. (39)]. This signal exhibits the well-known directional anisotropy between forward ($\epsilon = +1$) and backward ($\epsilon = -1$) scattering [Figs. 8(a) and 8(b)]. However, the areas of forward and backward change signals are equal. For high intensities ($s \gg 1$) $Q \simeq (s)^{1/2} = \beta/(\gamma_0\gamma_2)^{1/2}$, and we have

$$\Delta g(\tilde{v}_2, t=0, \epsilon) \simeq \frac{-(N_{20}/N_{10})g_0}{1+(\gamma_0/\gamma_2)[1-\epsilon(k_2/k_1)]} \times \mathrm{Re}\frac{\gamma(\epsilon)}{\gamma(\epsilon)+i\delta(\epsilon)}, \tag{61a}$$

with

$$\gamma(\epsilon) \simeq [(k_1/k_2)\gamma_{02} - \epsilon(\gamma_0/2)]Q. \tag{61b}$$

Thus, the change-signal amplitude saturates and its linewidth increases linearly with $\mathcal{E}_2^0$.

(ii) In a time of order of γ_B^{-1} the $e^{-(\gamma_B+i\delta)t}$ contribution vanishes, and both forward and backward signals are reduced to the same Lorentzian line shape,

$$\Delta g(\tilde{v}_2, t, \epsilon) \simeq \frac{-(N_{20}/N_{10})g_0}{1+(\gamma_0/\gamma_2)} \mathrm{Re}\left[\frac{\gamma_B-\gamma_0}{\gamma_B-\gamma_0+i\delta(\epsilon)}\right] e^{-\gamma_0 t}, \tag{62a}$$

with

$$\gamma_B - \gamma_0 \simeq (k_1/k_2)\gamma_{02}Q. \tag{62b}$$

(This result is valid even if phase-changing collisions occur.) As can be seen by comparing Eqs. (61) and (62), as the backward signal decays from $t=0$ its amplitude increases and its linewidth narrows, while the forward signal decreases and broadens! This behavior is clearly seen in Figs. 8(a), 8(b), and 9, where the time decay of forward

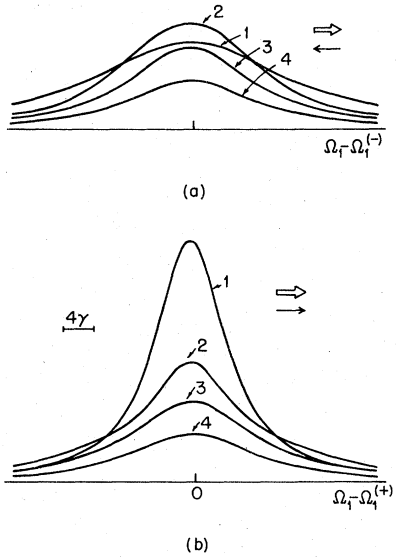

FIG. 8. Backward (a) and forward (b) change signals for strong saturation. The parameters are $k_1=k_2$, $N_{10}=N_{20}$, $\gamma_{ij}=\gamma$, and $\beta/\gamma=10$. Time delays: $t_1=0$, $t_2=0.2/\gamma$, $t_3=0.5/\gamma$, and $t_4=1/\gamma$.

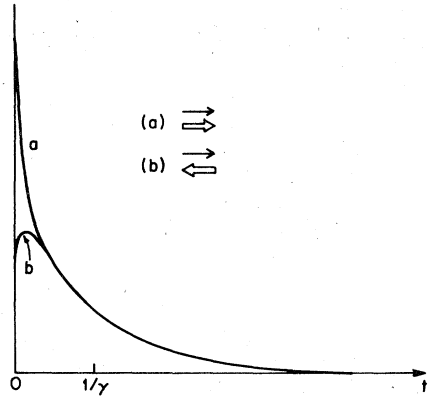

FIG. 9. Time decay of forward (a) and backward (b) change signals at line center ($\delta = 0$). The parameters are the same as in Fig. 8.

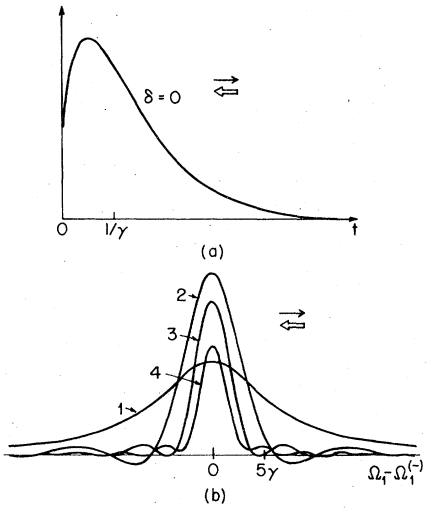

FIG. 10. Backward change signal for strong saturation and $k_1 \ll k_2$. The parameters are $k_1 = 0.1 k_2$, $\gamma_{ij} = \gamma$, and $\beta/\gamma = 10$. Time delays: $t_1 = 0$, $t_2 = 0.5/\gamma$, $t_3 = 1/\gamma$, and $t_4 = 2/\gamma$.

and backward change signals is plotted at line center.

This behavior occurs because in the steady-state the contribution from Raman-type processes broadens the backward change signal and narrows the forward one, as compared to the population saturation value. When the initial polarization (which contains the Raman contribution) has decayed away, in a time of order γ_B^{-1}, this influence is removed and the linewidths change. Furthermore, it follows from the equal-area property that rapid line narrowing automatically implies an increase in amplitude, and vice versa. Any process destroying the phase of the induced polarization—such as phase-changing collisions, Doppler dephasing or power dephasing—increases γ_B and thus accelerates the decay of the initial polarization. The remaining signal, due to population saturation, then decays away slowly with a time constant γ_0^{-1}.

Narrowing of this type has been reported by Shahin and Hänsch[21] in a time-delayed Lamb-dip experiment using a short-pulse dye laser. It should be noted that pulsed lasers are not ideal for such studies. The present method has the advantage that the system can be prepared in a well-defined steady state, and the weak cw field can precisely probe its decay.

Another interesting type of behavior can occur in the backward change signal when the initial saturation is large but $k_1 \ll k_2$ (reduced Doppler dephasing), so that $\gamma_B = \gamma_{01} + (k_1/k_2)\gamma_{02}Q$ is of the same order as γ_0. However, the initial linewidth $\gamma(-) \simeq \frac{1}{2}\gamma_0 Q$ is still power broadened [Eq. (39)]. In this case the decay rates of the initial polarization and the population are comparable, giving rise to narrowing at line center and Ramsey-type fringes at the wings. An example is given in Fig. 10. As can be seen, the central portion of the line narrows from $\gamma(-)$ to γ_B, with a corresponding increase in amplitude, in a time of order γ_B^{-1}, and narrow fringes appear at the wings of the resonance, in accord with Eq. (38).

B. Dynamical Stark splitting and oscillatory decay

When the two e.m. fields are co-propagating and k_2 is larger than k_1, a new steady-state feature appears at high saturating intensities: the resonance splits symmetrically into two distinct peaks.[26] As will be seen in the following, the decay of this signal exhibits a novel type of oscillatory behavior. The steady-state splitting has been observed recently by Toschek and co-workers.[38] Its lineshape features have been analyzed by Skribanowitz *et al.*,[39] particularly in the case of transitions with level degeneracy.

This type of behavior comes from the $\Delta g(\vec{v}_{12}, t, +)$ contribution, Eq. (41), which increases as $\beta^{1/2}$ at high intensities and thus predominates over the $\Delta g(\vec{v}_2, t, +)$ contribution, whose amplitude saturates. In the vicinity of the peaks Λ, Eq. (41b), is a slowly varying function proportional to iS, and so for $\beta \gg \gamma_{ij}$,

$$\Delta g(t,+) \propto \xi_{12}(t) = S \operatorname{Im} \frac{e^{-(\Gamma' + i\Delta')t/\kappa}}{\Gamma + i\Delta} \tag{63}$$

$$= S \frac{\Gamma \sin(\Delta' t/\kappa) + \Delta \cos(\Delta' t/\kappa)}{\Gamma^2 + \Delta^2} e^{-\Gamma' t/\kappa}. \tag{64}$$

The resonant behavior of the signal occurs through the denominator of Eq. (64). Using Eq. (42a) one

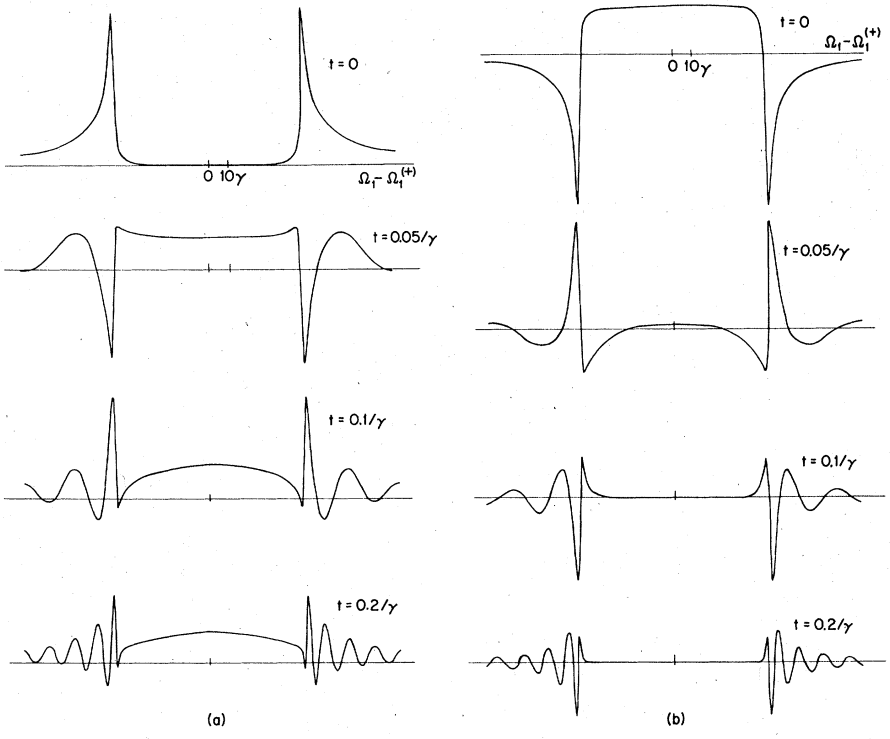

FIG. 11. Forward change signals for strong saturation, exhibiting dynamic Stark splitting. (a) N_{20} contribution; (b) N_{10} contribution. The parameters are $k_1=\frac{1}{2}k_2$, $\gamma_{ij}=\gamma$, and $\beta=10^4\gamma$. The time delays are as shown.

can show that[39]

$$\frac{1}{\Gamma^2+\Delta^2}=\frac{1}{(4\delta S)^{1/2}}\left(\frac{1}{\bar{\gamma}^2+(\delta-S)^2}-\frac{1}{\bar{\gamma}^2+(\delta+S)^2}\right)^{1/2}. \tag{65}$$

For $S\gg\bar{\gamma}$ this quantity undergoes a resonant enhancement around $\delta=+S$ (and a symmetrical one around $\delta=-S$):

$$(\Gamma^2+\Delta^2)^{-1}\simeq(2S)^{-1}[\bar{\gamma}^2+(\delta-S)^2]^{-1/2}. \tag{66}$$

Also note that in this vicinity Γ and Δ, Eq. (42a), can be approximated by

$$\Gamma\simeq S^{1/2}\{[(\delta-S)^2+\bar{\gamma}^2]^{1/2}-(\delta-S)\}^{1/2}, \tag{67}$$

and

$$\Delta\simeq S^{1/2}\{[(\delta-S)^2+\bar{\gamma}^2]^{1/2}+(\delta-S)\}^{1/2}. \tag{68}$$

As seen in Eq. (64) the steady-state ($t=0$) signal, proportional to $\Delta(\Gamma^2+\Delta^2)^{-1}$, exhibits two resonant peaks separated by $\simeq 2S$. The line shape of the $\delta=+S$ peak is given by

$$\xi_{12}(t=0)=\frac{S^{1/2}}{2}\left(\frac{[(\delta-S)^2+\bar{\gamma}^2]^{1/2}+(\delta-S)}{(\delta-S)^2+\bar{\gamma}^2}\right)^{1/2}. \tag{69}$$

This line shape is asymmetrical, the signal decreasing as $|\delta-S|^{-3/2}$ for $S>S-\delta\gg\bar{\gamma}$ and as $|\delta-S|^{-1/2}$ for $\delta-S\gg\bar{\gamma}$. The peak occurs at $\delta=S+\bar{\gamma}/\sqrt{3}$. Its amplitude is proportional to $S^{1/2}$ and its linewidth [full width at half maximum (FWHM)] is approximately $7\bar{\gamma}$.[40] This behavior is illustrated in the $t=0$ plots of Fig. 11.

The origin of this splitting lies in the high-frequency Stark effect[28] or "dynamical Stark splitting," which is caused by the mixing of the two wave functions of the energy levels of a transition saturated by a resonant e.m. field. In the optical region this frequency splitting is velocity dependent and is usually washed out by the Doppler effect. Thus, when averaged over a wide velocity distribution the splitting is transformed into a power broadening, which contributes to the linewidth of the resonance.[41] However, in the particular case considered here the velocity dependence can be substantially reduced over a wide velocity range, leading to the line shape splittings of Fig. 11.

The frequency features of the Stark splitting for a particular velocity group are determined by the resonant denominator $L_1L_{12}+\frac{1}{4}\beta^2$ appearing in the initial polarization $\Delta\sigma_{01}^{(1)}(0)$, Eq. (24). It can be written in the form

$$L_1L_{12}+\tfrac{1}{4}\beta^2=-(\Omega_1-\nu_+)(\Omega_1-\nu_-), \tag{70}$$

with $\nu_\pm$ the velocity-dependent center frequencies of the two Stark peaks. For $\beta\gg\gamma_{ij}$,

$$\nu_\pm(v)=\omega_1+k_1v+\tfrac{1}{2}[\Delta_2\pm(\Delta_2^2+\beta^2)^{1/2}], \tag{71}$$

with $\Delta_2(v)$, the detuning of the saturating field from

resonance,

$$\Delta_2 = \Omega_2 - \omega_2 - \epsilon k_2 v . \tag{72}$$

This resonant behavior is due to the coupling between σ_{01} and σ_{21}, as can be seen by determining their eigenfrequencies from Eq. (3) in the limit $\alpha \to 0$. A solution of the form $\sigma \propto e^{i\lambda t}$ gives

$$(\lambda - iL_{12})(\lambda - iL_1) = \tfrac{1}{4}\beta^2 , \tag{73}$$

which has roots (for $\beta \gg \gamma_{ij}$)

$$\lambda_\pm = -\Omega_1 + \nu_\pm . \tag{74}$$

The corresponding normal modes of the optical polarization P_1 oscillate at eigenfrequencies $\Omega_\pm(v) = \lambda_\pm + \Omega_1$ [see Eq. (2), ρ_{01} equation]. Resonant enhancement occurs when $\Omega(v)$ is Doppler shifted into resonance with the probe frequency. Setting $\Omega(v) = \Omega_1$, i.e., $\lambda = 0$, Eq. (73) then reduces to (70).[42]

For $k_1 > \epsilon k_2$ the velocity dependence of the term in brackets in Eq. (71) adds to the Doppler shift $k_1 v$. However, for $\epsilon = +1$ and $k_2 > k_1$ the velocity dependence of these two terms are opposite, leading to a partial cancellation of the velocity dependence of $\nu_\pm$. The resonant velocity groups contributing to the Stark splitting may be obtained from the condition $\Omega_1 = \nu_\pm(v)$. For the case $k_2 = 2k_1$ we have

$$k_1 v_\pm = \Omega_1^{(+)} - \omega_1 \pm (\delta^2 - S^2)^{1/2} . \tag{75}$$

(The considerations are similar for $k_2 \neq 2k_1$.) For $|\delta| = |\Omega_1 - \Omega_1^{(+)}| \gg S$, $v_\pm$ varies linearly with Ω_1, but as $|\delta|$ approaches S the dependence is much weaker. In fact, near $|\delta| \simeq S$ the velocity groups $v_+ \simeq v_-$ are essentially independent of Ω_1 over an interval $\Delta v \simeq S/k_1$. The washout effect is thus diminished, since all of the velocity groups in this interval can contribute to the high-frequency Stark resonance occurring at the corresponding value of Ω_1. This value is determined by the condition that the quantity $\delta^2 - S^2$ in Eq. (75) be close to zero,

$$|\delta| = S , \tag{76}$$

which gives the center frequencies of the Stark-split components [cf. Eq. (69)]. Note that because of the velocity dependence the Stark components are split by $2S$ rather than by 2β, as they would be in the homogeneously broadened case.[42,43] Also note from (75) that the resonance condition cannot be satisfied for any velocity group when Ω_1 is in the range

$$\Omega_1^{(+)} - S < \Omega_1 < \Omega_1^{(+)} + S . \tag{77}$$

This lack of resonant molecules explains why in this range of probe frequencies the molecular medium is nearly transparent to the probe. Outside this range there are always velocities satisfying $\Omega(v) = \Omega_1$, and the interaction of the probe with the molecular medium is nonvanishing.[44]

As can be seen in Eq. (64), when the saturating laser is terminated the resonance undergoes oscillations at frequency Δ'/κ as it decays with time constant Γ'/κ. In the vicinity of the resonance [Eqs. (42e)]

$$\Gamma' \simeq \tfrac{1}{2}\Gamma \tag{78}$$

where Γ is given by Eq. (67), and

$$\Delta' \simeq \tfrac{1}{2}S . \tag{79}$$

The number of oscillations is of the order of

$$\Delta'/\Gamma' \simeq (S/\bar{\gamma})^{1/2} . \tag{80}$$

Notice that this behavior is different from the well-known Rabi oscillations observed in optical nutation transients, since after $t = 0$ the saturating field is absent. The appearance of this new frequency is due to the dynamic Stark effect, which causes the resonant interaction between the molecules and the probe field to be shifted from $\Omega_1^{(+)}$ to a new value. When the saturating field is switched off, the v_- velocity group, prepared before $t = 0$, radiates at its natural frequency $\omega_1 + k_1 v_-$.[45] The reemitted field then beats with the probe field to give a beat at $\Omega_1 - \omega_1 - k_1 v_- = \Delta'/\kappa$.[46]

Some typical delayed line shapes are plotted in Fig. 11. A noteworthy feature is the distortion of the envelope of the decay curve, which enhances the outer shoulders of the resonance as the delay time increases. This effect occurs because the decay rate,

$$\Gamma'/\kappa \simeq (\sqrt{S}/2\kappa)\{[(\delta - S)^2 + \bar{\gamma}^2]^{1/2} - (\delta - S)\}^{1/2} , \tag{81}$$

is frequency dependent. This dependence is due to the fact, explained earlier, that the range of interacting velocities, and hence the Doppler-dephasing contribution to the decay, varies with Ω_1. It can be seen in Eq. (81) that the decay is faster on the inner sides of the resonance than on the outer sides. Thus, the asymmetry of the peaks is enhanced during the decay.

Figures 11(a) and 11(b) show the N_{20} and N_{10} contributions, respectively. Notice that while the N_{20} curve is initially transparent in the region between the Stark peaks (i.e., $|\delta| \ll S$), the N_{10} curve exhibits small gain over a broad region. The sign of this gain is opposite to that of the Stark peaks, as it must be to maintain zero area. After a short time delay ($t \sim S^{-1}$) the situation is reversed, the N_{20} curve exhibiting a broad central gain region and the N_{10} curve becoming transparent there. Also note that the area of the N_{10} curve remains zero throughout the decay, as it must.

The change-signal expression in this region can be obtained by considering Eqs. (31) and (41) in the limit $|\delta| \ll S$. For example, in the case of no phase-changing collisions, $k_2 = 2k_1$ and γ_0

$=\gamma_2$ [Eqs. (38) and (43)] one finds

$$\Delta g(t,+) = -g_0 e^{-St} + \frac{g_0}{2}\frac{N_{20}}{N_{10}}(e^{-St} - e^{-\gamma_0 t}), \tag{82}$$

which exhibits the features discussed above.

Finally, notice that whereas all contributions associated with the decay of initial polarization exhibit power dephasing for $\beta \gg \gamma_{ij}$, the contributions associated with population decay do not. Therefore, for very long delays ($t \sim \gamma_0^{-1}$) the line-splitting disappears. The remaining broad N_{20} contribution decays as $e^{-\gamma_0 t}$ (population effect) and evolves similarly to the backward resonance (Sec. V A).

VI. TIME-DELAYED FLUORESCENCE CHANGE SIGNALS

Three-level free-decay resonances can also be observed by monitoring the side fluorescence originating from level 1 as the probe field is tuned through the 0-1 transition. As explained in Sec. II B, the fluorescence intensity I_F is directly proportional to $\langle\sigma_{11}\rangle$, the velocity-integrated population of level 1 [Eq. (10)]. Thus, this type of experiment directly measures the time evolution of the level population changes induced by the probe field. For a weak probe these occur in second order in α. We will now calculate $\langle\sigma_{11}^{(2)}\rangle$ for a saturating field of arbitrary β.

A. Calculation of $\langle\sigma_{11}\rangle$

In the second order in α, σ_{11} is determined by Eq. (16). The solution can be written in the form

$$\sigma_{11}^{(2)}(t) = -\tfrac{1}{2}\alpha^2(\gamma_{01}/\gamma_1)(n_{10}/|L_1|^2) + \Delta\sigma_{11}^{(2)}(t), \tag{83}$$

where the first term describes the time-independent population change induced by the probe field. The second term, which describes the modification of the 0-1 transition rate induced by the saturating field, satisfies

$$\Delta\dot{\sigma}_{11}^{(2)} + \gamma_1\Delta\sigma_{11}^{(2)} = \tfrac{1}{2}i\alpha\Delta\sigma_{01}^{(1)}(t) + \text{c.c.}, \tag{84}$$

where $\Delta\sigma_{01}^{(1)}(t)$ is given by Eq. (26). The resulting expression for $\langle\sigma_{11}(t)\rangle$, complete up to order α^2, can then be written in the form

$$\langle\sigma_{11}(t)\rangle = \bar{n}_1 - \Delta\bar{n}_1^0 + \Delta\bar{n}_1(t,\epsilon), \tag{85}$$

with $\Delta\bar{n}_1^0$ the broad Gaussian background population change induced by the probe field for $\beta = 0$,

$$\Delta\bar{n}_1^0 = \alpha^2 N_{10}/2k_1\gamma_1,$$

and $\Delta\bar{n}_1(t,\epsilon) = \langle\Delta\sigma_{11}^{(2)}\rangle$ the population change signal.

One way of obtaining $\Delta\bar{n}_1$ would be to solve Eq. (84) and then integrate the resulting expression over the velocity distribution. A simpler approach is to integrate Eq. (84) over velocity, thus obtaining an expression relating $\Delta\bar{n}_1$ to Δg:

$$\Delta\dot{\bar{n}}_1 + \gamma_1\Delta\bar{n}_1 = -\gamma_1\Delta\bar{n}_1^0\Delta g(t,\epsilon)/g_0, \tag{86a}$$

where Eq. (28b) has been used. This equation has the solution

$$\Delta\bar{n}_1(t,\epsilon) = -\frac{\Delta\bar{n}_1^0}{g_0}\left(\Delta g(0,\epsilon)e^{-\gamma_1 t} + \int_0^t \Delta g(t',\epsilon)e^{-\gamma_1(t-t')}\gamma_1\,dt'\right). \tag{86b}$$

Thus the expression for the population change signal follows directly from that of the gain change signal, without the necessity of doing additional velocity integrals. As could be expected, the transient signal exhibits a new time constant γ_1^{-1} related to the relaxation of the population of level 1.

1. $k_1 - \epsilon k_2 \geq 0$

In this case Eq. (31) is used in (86b) to obtain

$$\Delta\bar{n}_1(\tilde{v}_2,t,\epsilon) = \Delta\bar{n}_1^0\left(\frac{k_1}{2k_2}\frac{\beta^2}{\gamma_0^2 Q}\frac{N_{20}}{N_{10}}\right)\mathrm{Re}\,\gamma_0\gamma_1\left[\frac{L_N + \frac{1}{2}\gamma_0(1+\epsilon Q)}{L_B L_N + \frac{1}{4}\beta^2}\left(\frac{e^{-\gamma_1 t}}{\gamma_1} + \frac{e^{-\gamma_1 t} - e^{-L_B t}}{L_B - \gamma_1}\right) - \frac{1}{L_B - \gamma_0}\left(\frac{e^{-\gamma_1 t} - e^{-L_B t}}{L_B - \gamma_1} - \frac{e^{-\gamma_1 t} - e^{-\gamma_0 t}}{\gamma_0 - \gamma_1}\right)\right]. \tag{87}$$

In Eq. (87) the complex Lorentzian denominators L_B and L_N have been introduced to simplify the form of the expression,

$$L_B = \gamma_B + i\delta(\epsilon), \quad L_N = \gamma_N + i\delta(\epsilon), \tag{88}$$

with γ_B and γ_N given by Eqs. (36) and (37), respectively.

2. $k_1 - \epsilon k_2 < 0$

In this case Eq. (41), used in (86b), leads to

$$\Delta\bar{n}_1(t,+) = \Delta\bar{n}_1(\tilde{v}_2,t,+) + \Delta\bar{n}_1(\tilde{v}_{12},t,+), \tag{89}$$

with

$$\Delta\bar{n}_1(\tilde{v}_{12},t,+) = \tfrac{1}{2}\Delta\bar{n}_1^0 S^2\ \mathrm{Re}\left[\frac{\gamma_1}{(\Gamma + i\Delta)\Lambda}\left(\frac{e^{-\gamma_1 t} - e^{-(\Gamma'+i\Delta')t/\kappa}}{(\Gamma' - \kappa\gamma_1 + i\Delta')/\kappa} + \frac{e^{-\gamma_1 t}}{\gamma_1}\right)\right]. \tag{90}$$

The notation used in Eq. (90) is the same as in Eqs. (41) and (42).

As can be seen in Eqs. (87) and (89), the steady-state line-shape behavior of $\Delta\bar{n}_1(t,\epsilon)$ is identical to that of $\Delta g(t,\epsilon)$. [This follows from Eq. (86a) with $\Delta\dot{\bar{n}}_1=0$. See also the discussion following Eq. (16).] However, the time-delayed line shapes are not the same. In the following, the $\Delta\bar{n}_1(t,\epsilon)$ change signals are analyzed in the limits of weak and strong saturation of E_2.

B. Weak field response

1. $k_1 \gg \epsilon k_2$

The response for $\beta \ll \gamma_{ij}$ is obtained by setting $\beta=0$ and $Q=1$ in Eq. (87), and replacing L_B and L_N by their unsaturated values,

$$L_B^0=\gamma_B^0+i\delta(\epsilon), \quad L_N^0=\gamma_N^0+i\delta(\epsilon), \tag{91}$$

with γ_B^0 and γ_N^0 defined as in Eqs. (50) and (51).

For counter-propagating waves, $\Delta\bar{n}_1$ is independent of L_N^0, indicating the cancellation of Raman-type processes. For $\epsilon=-1$ the term in brackets in Eq. (87) becomes

$$\zeta(-)=\frac{1}{L_B^0}\left(\frac{e^{-\gamma_1 t}}{\gamma_1}+\frac{e^{-\gamma_1 t}-e^{-L_B^0 t}}{L_B^0-\gamma_1}\right) - \frac{1}{L_B^0-\gamma_0}\left(\frac{e^{-\gamma_1 t}-e^{-L_B^0 t}}{L_B^0-\gamma_1}-\frac{e^{-\gamma_1 t}-e^{-\gamma_0 t}}{\gamma_0-\gamma_1}\right). \tag{92}$$

In the co-propagating case, $\Delta\bar{n}_1$ is given by Eq. (87) with $\epsilon=+1$. This expression dramatically simplifies when phase-changing collisions are absent, in analogy with the $\Delta g(t,+)$ change signal [see Eq. (55)]. We then have

$$L_B^0=L_N^0+\gamma_0, \tag{93}$$

and so the quantity in brackets in Eq. (87) reduces to

$$\zeta(+)=\frac{1}{\gamma_1 L_N^0}\left(\frac{\gamma_0 e^{-\gamma_1 t}-\gamma_1 e^{-\gamma_0 t}}{\gamma_0-\gamma_1}\right). \tag{94}$$

As in the $\Delta g(t,+)$ change signal, the influence of Doppler dephasing is absent, but the decay of the $\Delta\bar{n}_1(t,+)$ change signal is governed by γ_1, as well as by γ_0. For the special case $\gamma_0=\gamma_1$ the quantity in parentheses in Eq. (94) reduces to $(1+\gamma_1 t)e^{-\gamma_1 t}$.

Next, consider the case of strong phase-changing collisions and close transition frequencies ($\omega_1 \simeq \omega_2$), treated for Δg in Sec. IV C. In this limit,

$$\gamma_1\zeta(\epsilon)=\frac{\gamma_0 e^{-\gamma_1 t}-\gamma_1 e^{-\gamma_0 t}}{(\gamma_0-\gamma_1)L_B^0}+\frac{1+\epsilon}{2}\frac{\gamma_0 e^{-\gamma_1 t}}{\gamma_B^0 L_N^0}. \tag{95}$$

Just as in the Δg change signals, Eq. (60), the first term of Eq. (95) describes a broad population-saturation resonance of width $\gamma_B^0=\gamma_{01}+\gamma_{02}$, while the second term is a narrow resonance, width γ_{12}, induced by Raman-type processes. But in contrast to the narrow resonance of Δg change signal, which decays rapidly at the rate γ_B^0, the narrow contribution of $\Delta\bar{n}_1$ decays at the much slower rate γ_1. This difference occurs because the narrow contribution to the $\Delta\bar{n}_1$ change signal is caused by the buildup of population in level 1 due to the completion of $2\rightarrow 1$ and $0\rightarrow 1$ Raman-type transitions.[22] Although the information about these processes is contained in both the initial polarization $[\sigma_{01}^{(1)}(0)]$ and population $[\sigma_{11}^{(2)}(0)]$, the latter contribution is dominant when the polarization relaxation rate is rapid. Thus, the narrow $\Delta\bar{n}_1$ component decays at the population decay rate. This implies that the backward-forward asymmetry cannot be eliminated during the decay of the fluorescence change signal, in contrast to the behavior of the probe-field decay signal. Also note that the fluorescence change signal is not a simple exponential, and depends on the population relaxation rates of both levels 0 and 1.

2. $k_1 < \epsilon k^2$

For co-propagating waves there is an additional contribution to $\Delta\bar{n}_1$ for $k_2>k_1$, which may be obtained from Eq. (90) using Eq. (52). Just as in the Δg change signal, this term arises from Raman-type transitions, which can lead to a population buildup in level 1. Thus, it can occur even when there is complete transparency at the saturating field ($N_{20}=0$). In this case the $\Delta\bar{n}_1$ change signal is proportional to the real part of

$$\frac{N_{10}}{(\bar{\gamma}+i\delta)(\bar{\gamma}-\kappa\gamma_1+i\delta)}\left[e^{-\gamma_1 t}-\frac{\kappa\gamma_1}{\bar{\gamma}+i\delta}e^{-(\bar{\gamma}+i\delta)t/\kappa}\right]. \tag{96}$$

As compared to the corresponding Δg change signal, Eq. (58), Eq. (96) contains an additional term associated with the $\sigma_{11}^{(2)}(0)$ contribution, which decays at a rate γ_1. Thus, although the two change signals are identical at $t=0$, the fringes occurring in the time-delayed Δg change signals are less pronounced in the corresponding $\Delta\bar{n}_1$ signals.

C. Saturation effects

At high saturation intensities the decay rate of the initial polarization is very large due to power dephasing. Thus, all of the terms in Eqs. (87) and (90) associated with the initial polarization are diminished since, as compared to the corresponding Δg expressions, each term has an extra factor in the denominator proportional to the polarization decay rate.[47] Accordingly, for $\beta \gg \gamma_{ij}$ the time evolution of the $\Delta\bar{n}_1$ change signals is completely determined by the terms decaying at the population relaxation rates. Equations (87) and (90) thus reduce to

$$\Delta\bar{n}_1(\tilde{v}_2, t, \epsilon) = \Delta\bar{n}_1^0\left(\frac{k_1}{k_2}\frac{\gamma_1\gamma_{02}Q}{1+\gamma_0/\gamma_2}\frac{N_{20}}{N_{10}}\right) \times \mathrm{Re}\left(\frac{L_N+\frac{1}{2}\epsilon\gamma_0 Q}{L_B L_N+\frac{1}{4}\beta^2}\frac{e^{-\gamma_1 t}}{\gamma_1} + \frac{1}{L_B}\frac{e^{-\gamma_1 t}-e^{-\gamma_0 t}}{\gamma_0-\gamma_1}\right), \quad (97)$$

$$\Delta\bar{n}_1(\tilde{v}_{12}, t, +) = \tfrac{1}{2}\Delta\bar{n}_1^0 S^2\,\mathrm{Re}\left(\frac{1}{(\Gamma+i\Delta)\Lambda}\right)e^{-\gamma_1 t}. \quad (98)$$

The disappearance of the contribution associated with the initial polarization is responsible for the following differences in the behavior of the $\Delta\bar{n}_1$ change signal, as compared to that of the Δg change signal discussed in Sec. V: (i) There are no rapidly decaying terms. (ii) The forward-backward asymmetry does not decrease as the $\Delta\bar{n}_1$ change signals decay. (iii) In the $\Delta\bar{n}_1(\tilde{v}_{12}, t, +)$ change signal, which gives rise to the dynamical Stark splitting, the Stark peaks decay slowly. The line-shape deformation and oscillatory behavior characteristic of the $\Delta g(\tilde{v}_{12}, t, +)$ change signal are absent.

VII. CONCLUSION

This paper has presented a theoretical analysis of the change signals induced by the free-induction decay of a Doppler-broadened molecular transition, observed as a weak probe field is tuned through a coupled transition. The evolving line shapes can be studied either by monitoring the gain at the coupled transition or by studying the side fluorescence. As has been shown, the time-delayed change signals manifest a rich range of features including forward-backward line-shape asymmetries, Doppler-dephasing effects, Ramsey-type fringes, power broadening and dephasing, and dynamical Stark splittings exhibiting oscillatory decay. It was also shown that the time-delayed line shapes provide a unique way of distinguishing population saturation effects from Raman-type processes, owing to their different decay times.

The experimental observation of time-delayed change signals of the type discussed here requires that the saturating field be terminated in a time τ which is small compared to the characteristic decay times of the optical polarization,

$$\tau \ll \gamma_B^{-1}, \beta^{-1}, \quad (99)$$

(conditions for validity of the sudden approximation). Otherwise, the initially prepared polarization cannot freely decay, and instead will tend to follow the time behavior of the saturating field. If, however, $\tau < \gamma_i^{-1}$, the change-signal contribution associated with the saturated level populations will still decay at its characteristic rate.

In the present study the applied fields have been assumed to fall within the Doppler profiles of their respective transitions:

$$|\delta_j| < k_j u,$$

with $\delta_j = \Omega_j - \omega_j$ the detuning of E_j from the 0-j molecular center frequency. Thus, the Raman-type processes occur in the presence of a resonant intermediate state. However, the two-photon (Raman) condition can be satisfied even if the intermediate state is nonresonant, i.e., for

$$|\delta_j| > k_j u. \quad (100)$$

in this limit, certain simplifications occur. For example, the velocity spread of the molecules can be ignored in the single-quantum resonant denominators (L_1 and L_2), since $|k_j v| \ll |\delta_j|$ for all velocities. Furthermore, for a given value of β the transition probabilities for both single- and double-quantum processes are reduced. However, the double-quantum transitions (i.e., Raman-type processes involving the exchange of *two* quanta with the radiation fields[22]) predominate, so the buildup of population in the intermediate state is small. Thus, unlike the case of a resonant intermediate state, there is no interference between single- and double-quantum events, and the form of the change signals is simplified.[29] However, when the intermediate state is nonresonant an additional condition must be satisfied in order for the sudden approximation to hold,

$$\tau \ll |\delta_j|^{-1}. \quad (101)$$

Otherwise, the induced polarization will tend to respond adiabatically to the saturating field. In practice, Eqs. (100) and (101) are difficult to fulfill simultaneously, since they require $\tau \ll (ku)^{-1}$. However, the regime in which

$$|\delta_j|^{-1} \ll \tau \ll \gamma_i^{-1} \quad (102)$$

is readily acheivable. In this case the contribution to the change signal coming from the initially prepared polarization will adiabatically follow the saturating field,[48] and so will vanish when $E_2 \to 0$, but the population contribution persists and will decay at its characteristic rate.

Several recent publications have investigated the transient behavior of cascade and folded three-level systems when the two-quantum (or Raman) transition is resonant or near-resonant and condition (102) is satisfied. Theoretical studies[17,19] have shown that in this limit the equations of motion simplify and reduce to those of an effective two-level system, so that the time evolution can be described by a vector model in which a two-photon Bloch vector precesses about an effective field. Experiments[18,49,50] have verified the different

time behavior expected from the double-quantum (Raman) and single-quantum ("stepwise") processes. Their different frequency behavior has also been studied experimentally.[51]

In summary, when the intermediate state is nonresonant and the adiabatic approximation holds the theoretical description simplifies, resulting in relatively simple line shapes. Double-quantum transitions predominate over stepwise processes and all information about the relaxation of the initially prepared polarization is lost. There is no interplay between population-saturation effects and Raman-type processes. Thus, the backward change signal is negligible compared to the forward signal.[52] On the other hand, when the intermediate state is resonant the line shapes, which are more complicated, give rise to a richer range of effects, including detailed information about the polarization decay and other relaxation processes.

The fundamental premise of this paper, the time-delayed probing of a resonance line shape, is a basic one in quantum mechanics. The idea of preparing a system in a given initial state and then probing it at a later time goes directly to the process of quantum measurement. Thus, time-delayed laser saturation spectroscopy can provide a direct analysis of the dynamics of atomic and molecular systems—scattering and diffusion mechanisms, thermalization in the gaseous phase by velocity-changing collisions and radiative transfer, laser interactions, and M-changing collisions in degenerate systems[13,35] can all be studied. The extension to four-level systems, where pump and probe transitions have no common level, should lead to similar information about inelastic collisions.

ACKNOWLEDGMENTS

We wish to thank Claude Cohen-Tannoudji for several stimulating discussions on this subject, and Dan Seligson for preparing the computer figures. One of us (M.D.) wishes to thank Ali Javan and Michael Feld for their kind hospitality during his stay at MIT. One of us (M.S.F.) wishes to acknowledge support from the Alfred P. Sloan Foundation. This work was supported in part by the National Science Foundation and the U.S. Army Research Office (Durham).

APPENDIX: POLES OF $(L_1L_{12}+\frac{1}{4}\beta^2)^{-1}$

This appendix analyzes the solutions of the equation

$$L_1L_{12}+\tfrac{1}{4}\beta^2=0\,, \tag{A1}$$

where L_1 and L_{12} are given by Eqs. (4). Equation (A1) can be written in the form

$$(x-\delta_1+i\gamma_{01})(\chi x+\delta_{12}-i\gamma_{12})+\tfrac{1}{4}\beta^2=0\,, \tag{A2}$$

where

$$\delta_i=\Omega_i-\omega_i\,,\quad \delta_{12}=\delta_1-\delta_2\,, \tag{A3}$$

$$\chi=(\epsilon k_2-k_1)/k_1\,, \tag{A4}$$

$$x=k_1v\,. \tag{A5}$$

The solution of Eq. (A2) is straightforward,

$$x_\pm(\beta)=\tfrac{1}{2}\left[\delta_1-\frac{\delta_{12}}{\chi}-i\left(\gamma_{01}-\frac{\gamma_{12}}{\chi}\right)\right.$$
$$\left.\pm\left\{\left[\delta_1+\frac{\delta_{12}}{\chi}-i\left(\gamma_{01}+\frac{\gamma_{12}}{\chi}\right)\right]^2-\frac{\beta^2}{\chi}\right\}^{1/2}\right]. \tag{A6}$$

The sign of the complex square root is determined by the condition

$$x_+(\beta\to 0)=\delta_1-i\gamma_{01}\,,\quad x_-(\beta\to 0)=(-\delta_{12}+i\gamma_{12})/\chi\,, \tag{A7}$$

as required by Eq. (A2). Thus, for $\beta\to 0$ the quantity in curly brackets must approach

$$(\delta_1+\delta_{12}/\chi)-i(\gamma_{01}+\gamma_{12}/\chi)\,.$$

The sign of $\mathrm{Im}(x)$ gives the position of the corresponding pole in the complex k_1v plane. $\mathrm{Im}[x_+(0)]$ is always negative, whereas the sign of $\mathrm{Im}[x_-(0)]$ is the same as that of χ. Since $x(\beta)$ is determined by continuity from $x(0)$, $\mathrm{Im}(x)$, a continuous function of β, can change sign only if it vanishes for a given value of β. It is easily shown that Eq. (A2) cannot have a real solution, since γ_{01} and γ_{12} are always positive. Thus $\mathrm{Im}[x_+(\beta)]$ is always negative and $\mathrm{Im}[x_-(\beta)]$ has the sign of χ.

As explained in Sec. III B of the text, only the poles of x lying in the upper half of the complex plane can contribute in the velocity integrations. Thus, the x_+ pole never contributes, and the x_- pole can contribute only for $\chi>0(\epsilon=+1, k_2>k_1)$.[24(a)]

Using the definitions of δ, $\bar{\gamma}$ and κ introduced in the text, this pole can then be written in the form

$$x_-(\beta)=k_1\tilde{v}_{12}=\frac{1}{2\kappa}\left\{\left(\kappa\delta_1-\frac{k_1}{k_2}\delta_{12}\right)-i\left(\kappa\gamma_{01}-\frac{k_1}{k_2}\gamma_{12}\right)\right.$$
$$\left.+i[(\bar{\gamma}+i\delta)^2+S^2]^{1/2}\right\}. \tag{A8}$$

*This work was performed while the author was a Visiting Scientist at MIT.

†Present address: Univ. Fed. de Pernambuco, Recife-Brazil.

[1]W. E. Lamb, Jr., Phys. Rev. 134, 1429 (1964); A. Szöke and A. Javan, Phys. Rev. Lett. 10, 521 (1963); R. A. McFarlane, W. R. Bennett, and W. E. Lamb, Jr., Appl. Phys. Lett. 2, 189 (1963).

[2]P. H. Lee and M. L. Skolnik, Appl. Phys. Lett. 10, 303 (1967); R. L. Barger and J. L. Hall, Phys. Rev. Lett. 22, 4 (1969); N. G. Basov, I. N. Kompanets, V. S. Letokhov, and V. V. Nikitin, Zh. Eksp. Teor. Fiz. Pis. Red. 9, 568 (1969) [JETP Lett. 9, 345 (1969)].

[3]For a review, see P. E. Toschek in *Spectroscopie sans Largeur Doppler de Systèmes Moléculaires Simples*, Colloque No. 217 (CNRS, Paris, 1974), pp. 13–27; and V. S. Letokhov and V. P. Chebotaev, *Nonlinear Laser Spectroscopy*, Vol. 4, edited by D. L. McAdam (Springer, Berlin, 1977).

[4]G. E. Notkin, S. G. Rautian, and A. A. Feoktistov, Zh. Eksp. Teor. Fiz. 52, 1673 (1967) [Sov. Phys. JETP 25, 1112 (1967)]; M. S. Feld and A. Javan, Phys. Rev. 177, 540 (1969); T. Hänsch and P. Toschek, Z. Phys. 236, 213 (1970); B. J. Feldman and M. S. Feld, Phys. Rev. A 5, 899 (1972).

[5]R. H. Cordover, P. A. Bonczyk, and A. Javan, Phys. Rev. Lett. 18, 730 (1967); H. K. Holt, Phys. Rev. Lett. 20, 410 (1968); T. Hänsch, R. Keil, A. Schabert, and P. Toschek, Z. Phys. 266, 293 (1969); I. M. Beterov and V. P. Chebotaev, Zh. Eksp. Teor. Fiz. Pis. Red. 9, 216 (1969) [JETP Lett. 9, 127 (1969)]; A. Schabert, R. Keil and P. Toschek, Opt. Commun. 13, 265 (1975); Appl. Phys. 6, 181 (1975).

[6]For a review, see M. S. Feld in *Fundamental and Applied Laser Physics*, edited by M. S. Feld, N. A. Kurnit, and A. Javan (Wiley, New York, 1973), pp. 369–420; and I. M. Beterov and V. P. Chebotaev in *Progress in Quantum Electronics* 3, edited by J. H. Sanders and S. Stenholm (Pergamon, Oxford, 1974).

[7]R. G. Brewer and R. L. Shoemaker, Phys. Rev. A 6, 2001 (1972).

[8]B. Hocker and C. L. Tang, Phys. Rev. 184, 356 (1969); R. G. Brewer and R. L. Shoemaker, Phys. Rev. Lett. 27, 631 (1971).

[9]N. A. Kurnit, I. D. Abella, and S. R. Hartmann, Phys. Rev. Lett. 13, 567 (1964); C. K. N. Patel and R. E. Slusher, Phys. Rev. Lett. 20, 1089 (1968).

[10]I. J. Lowe and R. E. Norberg, Phys. Rev. 107, 46 (1957); S. B. Grossman, A. Schenzle, and R. G. Brewer, Phys. Rev. Lett. 38, 275 (1977).

[11]Similar effects can also be achieved with Stark switching or laser-frequency switching techniques (Refs. 7, 8, 10). However, if the switching leaves the laser frequency inside the Doppler profile, additional effects due to interference between free decay and optical nutation can occur.

[12]M. Ducloy and M. S. Feld, J. Phys. Lett. (Paris) 37, L-173 (1976).

[13]J. R. R. Leite, M. Ducloy, A. Sanchez, D. Seligson, and M. S. Feld, Phys. Rev. Lett. 39, 1469 (1977). See also M. Ducloy and M. S. Feld in *Laser Spectroscopy III, Springer Series in Optical Sciences*, edited by J. L. Hall and J. L. Carlsten (Springer, Berlin, 1977), Vol. 7, pp. 243–257.

[14]R. L. Shoemaker and R. G. Brewer, Phys. Rev. Lett. 28, 1430 (1972); R. G. Brewer and E. L. Hahn, Phys. Rev. A 8, 464 (1973); 11, 1641 (1975).

[15]J. R. R. Leite, R. L. Sheffield, M. Ducloy, R. D. Sharma, and M. S. Feld, Phys. Rev. A 14, 1151 (1976).

[16]A. Corney and G. W. Series, Proc. Phys. Soc. Lond. 83, 207 (1964); W. Gornik, D. Kaiser, W. Lange, J. Luther, and H. H. Schultz, Opt. Commun. 6, 327 (1972); S. Haroche, J. A. Paisner, and A. L. Schawlow, Phys. Rev. Lett. 30, 948 (1973).

[17]D. Grischkowsky, M. Loy, and P. Liao, Phys. Rev. A 12, 2514 (1975).

[18]M. Bassini, F. Biraben, B. Cagnac, and G. Grynberg, Opt. Commun. 21, 263 (1977).

[19]E. Courtens and A. Szöke, Phys. Rev. A 15, 1588 (1977) and references therein; Y. R. Shen, Phys. Rev. B 9, 622 (1974).

[20]G. M. Dobbs, R. H. Micheels, J. I. Steinfeld, J. H. S. Wang, and J. M. Levy, J. Chem. Phys. 63, 1904 (1975).

[21]T. W. Hänsch, I. S. Shahin, and A. L. Schawlow, Phys. Rev. Lett. 27, 707 (1971); I. S. Shahin and T. W. Hänsch, Opt. Commun. 8, 312 (1973).

[22]The term "Raman-type processes," as used here, includes both single- and double-quantum processes. For a discussion of this point see the Feld article of Ref. 6.

[23]L. S. Vasilenko, V. P. Chebotaev, and A. V. Shishaev, Zh. Eksp. Teor. Fiz. Pis. Red. 12, 161 (1970) [JETP Lett. 12, 113 (1970)]; B. Cagnac, G. Grynberg, and F. Biraben, J. Phys. (Paris) 34, 845 (1973); for a review on Doppler-free two-photon spectroscopy, see N. Bloembergen and M. D. Levenson, in *High Resolution Laser Spectroscopy*, edited by K. Shimoda (Springer, Berlin, 1976); B. Cagnac, Ann. Phys. (Paris) 9, 223 (1975).

[24a]The way of transposing the results from the "V" configuration [Fig. 3(a)] to the other configurations ["inverted V", Fig. 3(b), or cascade, Fig. 3(c)] has been discussed in detail by Feld and Javan (Ref. 4, pp. 560–562, Appendices C–D and Table II). For the "inverted V" configuration, the results are essentially the same as for the "V" configuration (change of an over-all sign, to transpose absorption and stimulated emission). On the other hand, for cascade transitions, the cases of co-propagating ($\epsilon=+1$) and counter-propagating ($\epsilon=-1$) beams reverse. This means: (i) Two-photon absorption processes are important for *counter-propagating* beams (instead of Raman-type processes for *co-propagating* beams in "V" and "inverted V" configurations). (ii) In the velocity integration (Sec. III B), the important quantity is now $k_1+\epsilon k_2$, instead of $k_1-\epsilon k_2$. The resonant velocity group, $\tilde{v}_{12}$, [Sec. III B 2 and Eq. (A8)] contributes to the signal for $k_1+\epsilon k_2<0$ only. Then, for cascade transitions, the dynamic Stark splitting and related oscillatory decay (Sec. V B) appear for $\epsilon=-1$ and $k_2>k_1$.

[24b]A detailed calculation leading to Eqs. (3)–(9) is given in Ref. 15.

[25]W. Heitler, *The Quantum Theory of Radiation* (Oxford, Univ., London, 1960), Sec. 20; C. Cohen-Tannoudji, Ann. Phys. (Paris) 7, 423 (1962).

[26]B. J. Feldman and M. S. Feld, Phys. Rev. A 12, 1015 (1975).

[27]The velocity integration of signals observed in transient processes has been analyzed in Ref. 15. The reader is referred to this work for more detail. (See,

in particular, Sec. IV and the Appendix of Ref. 15).

[28]S. H. Autler and C. H. Townes, Phys. Rev. 100, 703 (1955).

[29]M. S. Feld and A. Javan, Ref. 4.

[30]Reference 26, Eq. (29) and footnote 23.

[31]N. F. Ramsey, *Molecular Beams* (Oxford Univ., London, England, 1956), p. 124.

[32]J. C. Bergquist, S. A. Lee, and J. L. Hall, Phys. Rev. Lett. 38, 159 (1977); M. M. Salour and C. Cohen-Tannoudji, Phys. Rev. Lett. 38, 757 (1977).

[33]I. J. Ma, J. Mertens, G. zu Putlitz, and G. Schütte, Z. Phys. 208, 352 (1968); G. Copley, B. P. Kibble, and G. W. Series, J. Phys. B 1, 724 (1968).

[34]Hänsch *et al.*, Ref. 5.

[35]See J. R. R. Leite, M. Ducloy, A. Sanchez, D. Seligson, and M. S. Feld, Phys. Rev. Lett. 39, 1465 (1977) and references therein. Also M. Ducloy and M. S. Feld, Ref. 13.

[36]M. Dumont, J. Phys. (Paris) 33, 971 (1972); M. Gorlicki and M. Dumont, Opt. Commun. 11, 166 (1974).

[37]In the experiments of Ref. 36 both Zeeman coherence and population saturation are destroyed by splitting the magnetic sublevels, whereas in the present technique the Raman coherence and population saturation are reduced as the probe field is detuned from resonance.

[38]A. Schabert, R. Keil, and P. Toschek, Ref. 5.

[39]N. Skribanowitz, M. J. Kelly, and M. S. Feld, Phys. Rev. A 6, 2302 (1972).

[40]Note that the linewidth value quoted in Ref. 39 is too small by a factor of 2.

[41]E. V. Baklanov and V. P. Chebotaev, Zh. Eksp. Teor. Fiz. 60, 552 (1971) [Sov. Phys. JETP 33, 300 (1971); 34, 490 (1972)] have interpreted the saturated absorption line shape in a Doppler-broadened transition in terms of the high-frequency Stark effect.

[42]This condition is derived in another way in C. H. Townes and A. L. Schawlow, *Microwave Spectroscopy* (McGraw-Hill, New York, 1955), Sec. 10-9.

[43]A. Javan, Phys. Rev. 107, 1579 (1957).

[44]The high-frequency Stark splitting appears naturally when the electromagnetic field is quantized and one looks for the energy levels of the total system, molecule plus field (formalism of the "dressed" molecule). C. Cohen-Tannoudji and collaborators recently have calculated the steady-state Doppler-averaged response using this formalism (C. Cohen-Tannoudji, private communication).

[45]The $v_\pm$ velocity groups are obtained from the equation $\Omega = \nu_\pm(v)$, as in Eq. (75). The oscillatory behavior comes from the v_- group. The pole associated with v_+ lies outside the contour in the complex v plane and does not contribute to the velocity integration.

[46]Using Eqs. (68) and (42e) one can show that

$$k_1 v_- = \Omega_1 - \omega_1 - \Delta'/\kappa.$$

[47]Note the similar effect caused by strong phase-changing collisions, which led to the simplified lineshape of Eq. (95).

[48]To ensure adiabaticity one also must have $|\delta_2| \gg \beta$. (See, for example, Courtens and Szöke, Ref. 19).

[49]D. Grischkowsky, Phys. Rev. A 14, 802 (1976).

[50]P. F. Williams, D. L. Rousseau, and S. H. Dworetsky, Phys. Rev. Lett. 32, 196 (1974).

[51]J. L. Carlsten and A. Szöke, Phys. Rev. Lett. 36, 667 (1976); J. Phys. B 9, L231 (1976).

[52]This statement holds for a folded system. In the case of a cascade configuration the *forward* signal is absent. This is because in the cascade case the roles of forward and backward signals are interchanged [see footnote 24a].